Investigating the role of the GCH1/AP-1 interaction and tetrahydrobiopterin in the regulation of oxidative stress within neurons

---

Adam Matthew Elkin

Masters By Research

University of York

Biology

December 2021

Abstract

Under conditions of stress, Reactive Oxygen Species (ROS) are generated. ROS are high energy damaging forms of oxygen molecules. Dysfunction of the organism's ability to adapt to changing levels of ROS, and accumulated ROS-related damage through the life-history can lead to the ageing and senescence, which has been suggested to contribute to the development of Parkinson's Disease and ALS. In neurons, ROS activates numerous cellular responses, including the activation of the Jun-N-terminal kinase (JNK) pathway, together with its target Activator Protein 1 (AP-1). How this response is regulated within neurons has yet to be clearly defined. In our model synapse, the *Drosophila* 3rd instar neuromuscular junction (NMJ), AP-1 positively regulates growth and strength while regulating ROS levels. A previous investigation into proteins that differentially bind to AP-1 during oxidative stress in *Drosophila* neurons identified Punch (Pu) (GTP cyclohydrolase-1). Punch is the first step in the synthesis for tetrahydrobiopterin (BH_4), a crucial oxidation sensitive cofactor with an important role in neurotransmitter synthesis and regulation of ROS. We hypothesise that in conditions of normoxia Punch is inhibited by high levels of BH_4 which promotes binding to and inhibition of AP-1. Punch was found bound to AP-1 in normoxic conditions, but not bound under conditions of oxidative stress, releasing AP-1 to function. Reducing the levels of Punch allows the release of AP-1 which drives synaptic overgrowth within the *Drosophila* NMJ under conditions of oxidative stress which can be reduced with anti-oxidant treatment or by raising BH_4 levels using Dihydrofolate Reductase (DHFR) overexpression, an enzyme that converts BH_2, the oxidised form of BH_4, back to BH_4. Our work dissects a novel mechanism tuning the response of AP-1 to increasing levels of ROS.

Covid19 Statement

This investigation was conducted throughout the pandemic, which did impact aspects of the project. The main impact was with reduced lab space leading to reduced time spent in the lab conducting experiments. More bioinformatics were conducted as a result of this. Another aspect of the pandemic impacted work was with training and time on epifluorescent and confocal microscopes. Training was delayed due to reduced capacity and work conducted on the epifluorescent microscope was dependent on lab capacity. Other aspects that were affected were deliveries for chemicals, both due to the Covid19 pandemic and Brexit. This mainly affected the delivery of Trolox and Amplex Red reagents.

Acknowledgements

I would like to express my sincere gratitude to my supervisors, Dr. Sean T Sweeney and Dr Sangeeta Chawla for giving me the opportunity to conduct this investigation and for their patience, motivation and support throughout my time as a Master's by Research student. I would not be where I am currently without their guidance and constant support, especially through these difficult times, for which I am sincerely grateful.

Along with my supervisors, I would also like to thank my TAP member, Dr Gonzalo Blanco, for his insightful suggestions and encouragement which helped to progress this investigation forward. For their help with experiments and data collecting, I would like to thank Stella Wigglesworth, Professor Tony J Wilkinson and Juliet Borgia.

Especially with the difficult times throughout the year, I would like to thank the members of the D1 block, Dr Chris J H Elliot, Alison Fellgett, Katy Hyde, Dr. Chris Ugbode, Egle Beigaite, Tim Johnston, Emily Sample and Kelly Roy, for their support and company throughout the entire year. I would also like to thank Dr Paul Pryor for his supervision and guidance throughout both my undergraduate and postgraduate time in York.

Finally, I would like to thank my friends and family for their constant support and company, making life so much easier throughout these difficult times. Of which I would like to express my sincere gratitude to my Mum, Kate Dudzinska, and Step-dad, Martin Fisher, who with their constant support and encouragement have got me to where I stand today.

Author's Declaration

I declare that this thesis is a presentation of original work and I am the sole author. This work has not previously been presented for an award at this, or any other, University. All sources are acknowledged as References.

Contents

Figure Contents

Table Contents

Chapter 1. Introduction

1.1 Effects of ageing and neurodegeneration on neurons

Early organisms evolved mechanisms of metabolism to utilise oxygen as an electron acceptor to efficiently produce adenosine triphosphate (ATP) as an energy source. This form of metabolism causes a leakage of Reactive Oxygen Species (ROS), a damaging high energy form of oxygen. This trade-off is present within all aerobic organisms. Aerobic organisms must trade off energy production against cellular damage. When ROS exceeds the capacity of the cell to constrain damage, it is termed Oxidative Stress. ROS leakage also contributes to the free radical theory of ageing [1]. Dysfunction of the organism's ability to adapt to changing levels of ROS, and accumulated ROS-related damage through the life-history can lead to the ageing of the organism, which has been suggested to contribute to the development of many diseases, including Parkinson's Disease and amyotrophic lateral sclerosis [2].

Due to the improvement in individual health outcomes and increased longevity, we are developing an ageing population with resultant increase in age-related diseases, including cardiovascular diseases, neurodegeneration and cancer [3,4]. The ageing process progressively worsens the function of tissues and organs at multiple levels, including changes to gene expression, metabolic control and most importantly the production of high levels of ROS and Reactive Nitrosative Species (RNS) [4,5]. The lack of knowledge into the processes of ageing prevents the development of therapies to prevent or delay age-related pathologies, which are becoming one of the greatest health threats of this generation [6].

Ageing develops from an accumulation of physical, environmental and social factors, indicating that there is not a single process to ageing, but a large number of independent, stochastic processes that lead to the accumulation of damage in parallel with each other [3,4]. One of the main factors that contributes to the ageing process are free radicals including ROS and RNS. These are highly reactive atoms or molecules with one or more unpaired electrons in their external shell, therefore behaving as oxidants or reductants which can cause oxidative damage [5,7]. These can be produced by several endogenous and exogenous processes, with the main source being the inefficient electron transfer in the mitochondrial respiratory chain, leading to an imbalance between ROS and the antioxidant defence mechanisms and as a result causes nonlinear cellular responses [4]. Oxidative stress has a central role in the neurodegenerative process, since the brain and neurons, which are rich in lipid content, have a high energy demand and weak antioxidant capacity, are targets for

oxidative damage [8]. Neurons also tend to accumulate dysfunctional and aggregated proteins due to oxidative imbalance, leading to poorer performance in several cognitive domains due to ageing [6,9].

Neurodegenerative diseases, including Parkinson's Disease (PD), Alzheimer's Disease (AD), Multiple Sclerosis (MS) and amyotrophic lateral sclerosis (ALS), all have excessive ROS as a contributor to pathology. They each cause conditions where the nerve cells from the brain or spinal cord are damaged and/or lost with a pathological hallmark of ROS-related damage, leading to either ataxia or dementia [10]. Specific brain regions exhibit different vulnerabilities in various diseases, for example neurons in the entorhinal cortex, hippocampal CA1 region and amygdala are most sensitive in association with Alzheimer's, while dopaminergic neurons of the substantia nigra are most sensitive in Parkinson's Disease, which reflects both the specificity of these diseases and the heterogeneity in the neuronal responses [11]. However, despite the extensive studies into each of these diseases, the mechanism of neurodegeneration is still poorly understood with the relative contribution of ROS still to be resolved.

1.2 Role of reactive oxygen species involvement in ageing and neurodegeneration

An unavoidable byproduct of aerobic metabolism is the production of ROS, which includes superoxide (O_2-), hydroxyl radicals (·OH) as well as nonradical molecules including hydrogen peroxide (H_2O_2) and singlet oxygen ($1O_2$) [12]. These molecules can be generated through a number of sources, including xenobiotics, cytokines, bacterial invasion and most predominantly from mitochondrial oxidative metabolism [13]. Despite the destructive activity of ROS being implicated in ageing and neurodegeneration, it also serves as a cell signaling molecule for a variety of cellular processes, including tolerance to environmental stresses, which indicates that it is necessary for cells to tightly control the levels of ROS through antioxidant defence mechanisms [12,14].

The generation of cellular ROS can be induced by both endogenous and exogenous stimuli, with processes causing uncoupling of the electron transport at the mitochondrial respiratory chain enhancing the production of ROS [14]. During mitochondrial respiration, electrons are released from the electron transport chain which incompletely reduces O_2 to form a superoxide that is further converted into H_2O_2 by manganese superoxide dismutase within the mitochondrial matrix [15]. The production of these superoxide anions primarily occurs at two points of the chain, complex I and complex III [16]. Although the mitochondria are the major source of intracellular ROS, other cellular components such as endoplasmic reticulum-bound enzymes, cytoplasmic enzyme systems and the cytochrome P450 monooxygenase system also increase the generation of ROS [14]. Iron, the most abundant metal in the body, also has the ability to generate oxidative stress through the action of Fenton reactions within organelles such as the lysosome [16]. However, over the past decades, evidence has shown that ROS also serves as a signaling molecule to regulate biological processes [17]. For example, the *Drosophila* MICAL (molecules interacting with CasL) protein, which is essential for regulating myofilament organisation and synaptic structures, acts directly on actin through ROS production [18]. This shows that ROS within cells must not be completely removed from the system, but kept at physiological levels to allow normal cellular function.

The free radical theory of ageing is based on the hypothesis that the age-related functional loss of tissues and organs is due to the accumulation of oxidative damage by ROS, which leads to damage to lipids, DNA and proteins [5]. This accumulation of oxidative stress has been linked to numerous neurological diseases, which are characterised by the progressive damage and loss of neuronal loss that may be exacerbated through ROS [19]. For example in Alzheimer's Disease, past studies have shown that oxidative damage does play a role in the loss of neurons and progression to dementia and also the generation of β-amyloid, a toxic peptide found in AD patient's brains [20]. There is also evidence that the nitration and nitrosylation of certain proteins and protein oxidative damage in the form of protein carbonyls within the brain of Parkinson's patients are due to RNS [21]. The pivotal role of oxidative stress in neurodegenerative diseases represents the need to further understand the mechanisms of oxidative damage and potentially represent a promising therapeutic therapy to slow down the development of neurodegeneration and its symptoms, along with other age-related diseases, but this must be balanced against the need for normal physiological signaling by ROS [19].

1.3 Protective neuronal mechanisms in response to ROS

Protection against ROS and oxidative stress is mediated by layered standing and adaptive forms of defence. For example in the brain, static defences include high concentrations of enzymes such as superoxide dismutase (SOD), thioredoxin reductase (Trx) and catalase (cats). These are front-line antioxidant enzymes responsible for regulating oxidative stress levels [22,23]. Protection can also be mediated by small organic defence molecules, such as alpha-tocopherol (vitamin E) and glutathione [24]. These mechanisms ensure that levels of ROS are kept at a basal level. However when levels of ROS increase, the cell deploys an adaptive antioxidant defence mechanism to respond to changes in increased oxidative stress.

The ability to induce cellular defence mechanisms in response to ROS is required in both eukaryotic and prokaryotic organisms to prevent loss of function in cellular systems due to free radicals [2,10]. Many of the system's cells deploy an antioxidant defence that can be rapidly controlled to fit the changing levels of oxidative stress [25]. This mechanism is highly important for cellular health, and the lack of cellular response can lead to the build up of ROS and lead to increased cellular damage.

There are two major protective mechanisms present within brains, the Nuclear factor erythroid 2-related factor 2 (NRF2)/Keap system which is predominant in glial cells [26], and the JNK/AP-1 system which controls the expression of many antioxidant genes, which has a critical antioxidant role in neurons [24]. Both of these pathways promote the adaptive transcription of antioxidant response proteins to tackle the changing levels of ROS, which is highly important within neurons and synapses that have higher levels of mitochondria to sustain the elevated levels of energy demand [8,16]. As this project focuses on mechanisms of ROS defence within neurons, we will focus on the JNK/AP-1 system.

1.4 The role of AP-1/JNK interaction in the antioxidant adaptive response

The transcription factor AP-1, which is mainly composed of Fos, Jun and ATF homo- and heterodimers, is required for normal motor neuron dendritic growth, both during development and response to activity induction [27,28]. Previous studies have shown that both AP-1 and NFkB are induced in response to oxidative stress and many other exogenous stimuli, including hypoxia and excitotoxicity, regulated by Serum Response Factor (SRF), cAMP response element-binding protein (CREB) and c-Jun [2,29]. As with other transcription factors, AP-1 has roles in inducing, suppression and modulation of transcription.

Oxidative stress activates numerous cellular responses, including the activation of the Jun-N-terminal kinase (JNK) pathway, which together with its target AP-1 to positively regulate growth and strength at the larval NMJ along with regulating ROS levels. In mammalian cortical neurons the antioxidant defence protein SRXN-1 is regulated in a c-Jun dependent manner [16,30]. JNK signaling also acts on many phosphorylation targets which have been implicated in learning and memory with critical roles in the growth and development of synapses and the stress response [29]. It has also been suggested that the JNK/AP-1 signaling pathway can induce synaptic overgrowth in *Drosophila* motor neurons through activation by ROS, and disrupting this pathway impacts redox homeostasis [30,31]. These mechanisms show that AP-1 mediated transcription is highly important for dendritic growth, long-term plasticity and apoptosis, which if disrupted can contribute to the development of numerous neurodegenerative diseases [27,28] but critically in neurons appears to be the major antioxidant adaptive response.

In the Sweeney lab, an investigation into the proteins that bind to AP-1 during oxidative stress within Drosophila neurons was carried out [32]. One protein, GTP cyclohydrolase 1 (GCH1/GTPCH1, known as Punch in *Drosophila*) was found bound to AP-1 in normoxic conditions, but not bound under conditions of oxidative stress. GTPCH1 is known to regulate the synthesis of the oxidation sensitive enzyme cofactor tetrahydrobiopterin (BH_4). Subsequent studies showed that BH_4 induced binding of GTPCH1 to AP-1 and inhibition of AP-1 activity. Oxidation of BH_4 reversed GTPCH1 binding to AP-1 and release of AP-1 activity. We aim in this project to further understand the role of this regulatory system in neuronal responses to ROS.

1.5 Tetrahydrobiopterin as a regulator of oxidative stress

To trigger an appropriate antioxidant response, the JNK/AP-1 system must be able to detect the levels of ROS present to ensure the balance of ROS is kept at physiological levels. Two potential sensor/triggers have been identified in previous studies, which include Glutathione S-transferase Pi (GSTp) and mammalian thioredoxin (Trx)[33,34]. In this study, we identify tetrahydrobiopterin as another potential sensor for the AP-1 system. Tetrahydrobiopterin (BH_4) is a crucial cofactor for numerous aromatic amino acid hydroxylases, including glyceryl-ether mono-oxygenase and phenylalanine-4-hydroxylase, and plays an important role in monoamine neurotransmitter synthesis [35,36]. It has also been long known as a critical regulator of nitric oxide synthase (NOS) and reactive oxygen species (ROS) production, with a deficiency of BH_4 leading to nitric oxide synthase uncoupling and the production of superoxide (O2-) rather than NO, which has implications the development of various pathological disorders [37,38]. Due to its oxidisable and substoichiometric nature, the quantification and analysis of BH_4 has not been truly achieved to a high sensitivity and applicability, which is needed to further understand the role of BH_4 and its therapeutic potential for various disorders, including Parkinson's Disease and cardiovascular disorders [36,39].

The biosynthesis of BH_4 has been extensively characterised in higher organisms, and is also well established and conserved in *Drosophila melanogaster* [35,40]. This ubiquitous, multifaceted molecule is synthesised from GTP in a 3-step reaction, which includes GTP cyclohydrolase (GTPCH1), 6-carboxytetrahydropterin (6-PTP) and 6-pyruvoyltetrahydropterin synthase (PTP synthase) [35]. GTPCH1, which exists as a homodecamer, is encoded by the *GCH1* locus and is the primary rate-limiting enzyme in the synthesis of BH_4 [41]. Within *Drosophila,* the genetically complex *Punch* locus encodes GTPCH1, which when mutated can affect the activity of GTPCH1 in the heads of adults [42,43]. In vertebrates, BH_4 regulates its own synthesis mediated by a regulatory subunit, the GTP cyclohydrolase feedback regulatory protein (GFRP), which inhibits the activity of GTPCH1 when GTP and BH_4 levels are high and BH_4 is bound to GFRP [44].

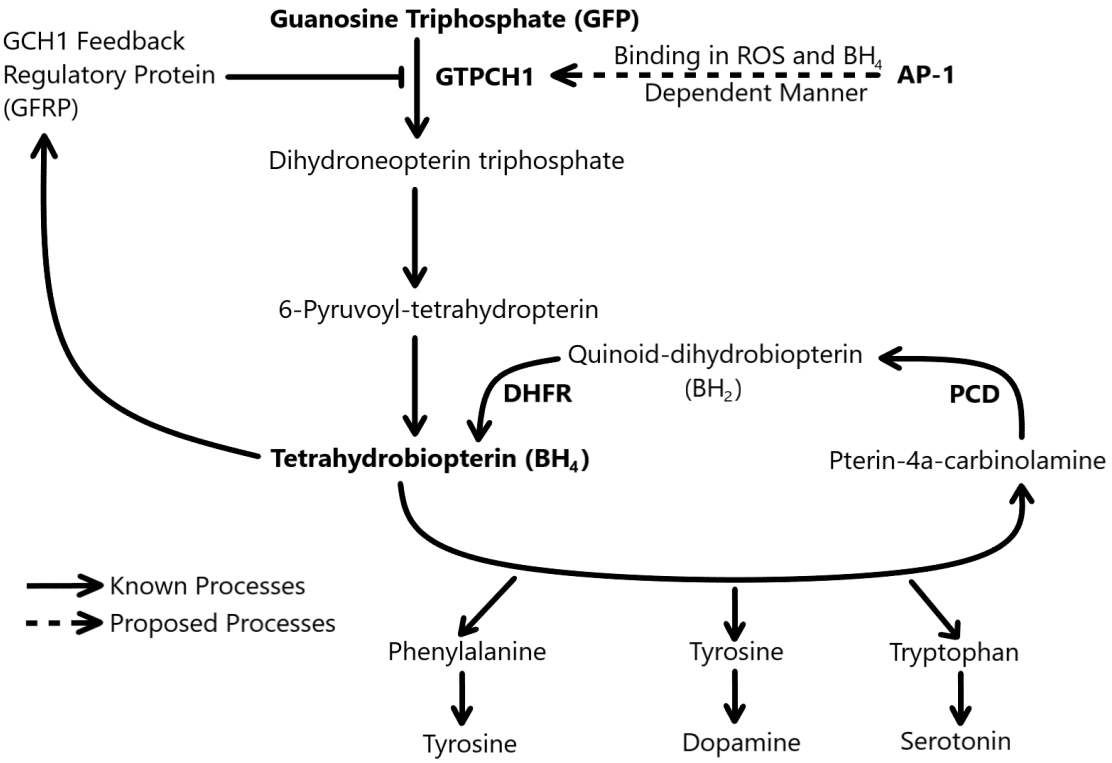

Figure 1. Known and proposed interactions between GTPCH1, BH_4 and AP-1

BH_4 is produced from GTP through the rate-limiting enzyme GTPCH1 followed by the function of pyruvoyl-tetrahydropterin synthase (PTPS). BH_4 is necessary for the synthesis of numerous monoamine neurotransmitters, including dopamine and serotonin. Indeed, mutations within the *GCH1* gene, including a novel DYT-5a mutation in exon 6 of the gene, have been shown as the fist causative mechanism for dopa-responsive dystonia, an autosomal dominant neurological disorder [47].

In mammals, the activity of GTPCH1 is inhibited by increased levels of BH_4 production through the activity of GCH1 feedback regulatory protein (GFRP), as shown in Figure 1. In *Drosophila*, this function of non competitive inhibition of Punch by BH_4 is conferred by an N-terminal extension of the protein [45,46]. In a previous study in the Sweeney laboratory (York), AP-1 has been shown to bind to GTPCH1 in a ROS and BH_4 dependent manner, which indicates the existence of a coupled mechanism where the oxidative state of BH_4 is linked to the transcriptional response of AP-1 [32].

Once synthesized, BH_4 is involved in a wide range of biological processes, including ether lipid metabolism and the synthesis of numerous neurotransmitters including dopamine, serotonin and noradrenaline [24,48]. For example, the synthesis of dopamine takes place in the cytosol of dopaminergic neurons, starting with tyrosine hydroxylase (TH), which generates tyrosine from the amino acid phenylalanine. TH is the first and rate limiting enzyme in the process, which requires BH_4 as an obligatory cofactor [49,50]. Therefore genetic defects in the enzymes responsible for the synthesis or regeneration of BH_4 can lead to a toxic build-up of L-phenylalanine and deficiency of dopamine and epinephrine, which are associated with the development of severe neurological disorders [36,37]. BH_4 can be readily oxidised to BH_2 through numerous mechanisms, including synthesis of neurotransmitters including dopamine [51]. Dihydrofolate reductase (DHFR) can recycle BH_2 to BH_4 and therefore regenerate the levels of BH_4 and restore its balance as shown in Figure 2.

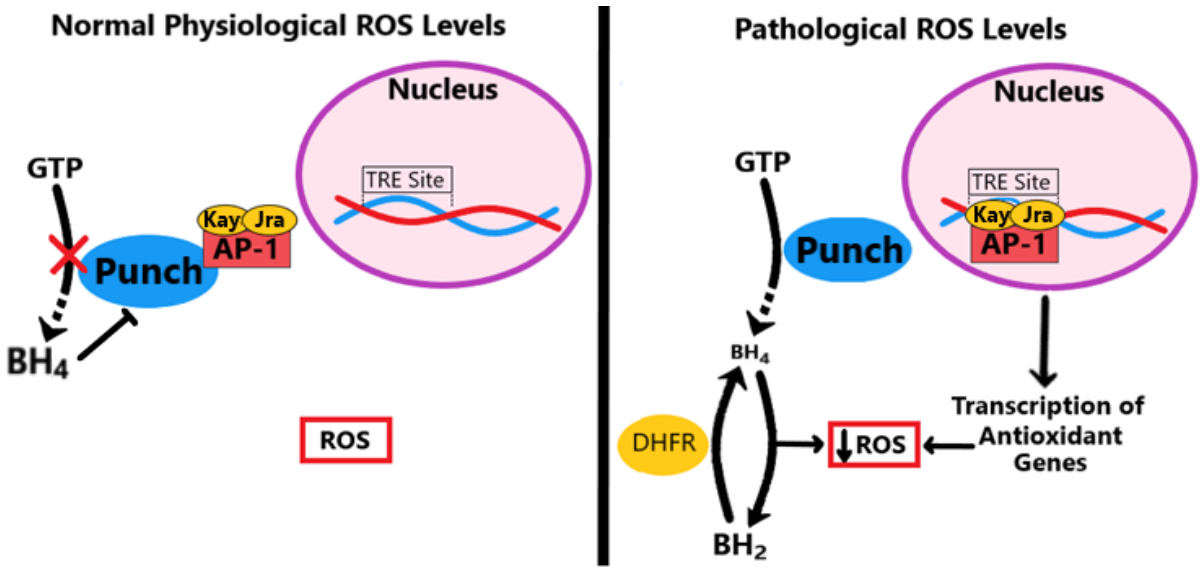

Figure 2. Negative regulation of oxidative response through AP-1/GTPCH1 binding

An investigation conducted by Nathan Garnham [32] showed binding of AP-1 subunits Fos and Jun to GTPCH1 during normoxic conditions but not during oxidative stress. We therefore hypothesised, and as outlined in this schematic, that during physiological conditions, AP-1 binds to GTPCH1, preventing the rate limiting step of BH_4 synthesis while also preventing AP-1 transcription within the nucleus. Oxidative stress via oxidation of BH_4 to BH_2 would cause the interaction between AP-1 and GTPCH1 to break, allowing for the synthesis of BH_4 and transcription of numerous antioxidant genes.

1.6 AP-1 regulation of neuromuscular junction growth via oxidative stress

Neuromuscular junctions (NMJ) serves as one of the best models for studying the formation of synapses, through changes in bouton count, branch number and synapse length [52]. Patterned synaptic activity leads to the activation of cyclic AMP response element-binding protein (CREB) which with cofactors leads to synaptic change [53]. It has been previously shown that AP-1 mediates long-term plasticity by functioning upstream of CREB to regulate bouton number and synaptic strength [53,54]. Oxidative stress has also been shown to induce synaptic overgrowth, through either *sod1* mutation or toxins, by the activation of synaptic growth pathways [31]. This ROS signaling is obligatory for the activation of multiple synaptic pathways, leading to neuronal activity dependent structural plasticity [55]. This further builds upon the proposed idea that ROS levels must be balanced to ensure normal physiological function within the system, allowing synaptic plasticity without the consequences of oxidative stress.

One pathway proposed in synaptic growth is the activation of JNK and Fos signaling. ROS is known to stimulate JNK which are known potent activators of synapse overgrowth and function [31]. Mutations in *Fos* rescued synaptic overgrowth within the late endosomal/lysosomal membrane protein spinster (*spin)* loss-of-function mutants, *sod1*, *sod2* and toxin treatment, which indicates that the JNK/AP-1 signaling is required for oxidative stress induced synapse overgrowth [31]. The past studies imply that not only does the JNK/AP-1 pathway have implications in regulating the antioxidant adaptive response, but it also regulates the synapse growth in response to the changing levels of ROS within the system. We therefore propose to investigate the implications of the Punch/AP-1/BH_4 interaction on neuromuscular junction growth under differing conditions of oxidative stress, through investigating changes in synapse overgrowth through bouton counts, branch number and synapse length.

1.7 *Drosophila* as a model organism for research

The fruit fly, *Drosophila melanogaster, is a* very versatile genetic model that has been used in modern biological science for the past 100 years, and to this day contributes to the future of regenerative medicine in many ways [56]. They are an excellent model to study essential genetic and cellular pathways for many human conditions, including ageing and neurodegeneration [57]. The genome of *Drosophila* is around 60% homologous to humans and around 75% of all genes responsible for human disease have a homolog in the *Drosophila* genome. The genome has been completely sequenced and annotated onto all 4 *Drosophila* chromosomes [58,59]. With their low cost of rearing and housing, limited ethics and rapid generation time as well as a range of genetic tools available for *Drosophila* make these organisms a powerful model to study for numerous diseases and pathways [60].

Each developmental stage of *Drosophila*, including the embryo, larvae, pupa and adult, have their own advantages for study [58]. For example, the third instar larva can be studied for developmental and physiological processes, dissected to study the *Drosophila* neuromuscular junction (NMJ) synapse and has simple behaviours such as crawling and foraging. The NMJ is an established model system, with 30 muscles per hemisegment arranged within the peripheral body that are used to study synaptic development and plasticity [61]. The relatively short life cycle of the fly means experiments including NMJ dissections can be completed in a matter of weeks, compared to other vertebrate models including mice and zebrafish which can take months or years to experiment with [56]. The availability of powerful genetic tools, including CRISPR reagents for genome editing and constructs for over-expressing or knocking down any gene in any tissues, allows genetic analysis to study and provide further insight into identified pathways or into the roles played by individual factors within a biological process [56,62].

This potential of genetic approaches makes flies a very powerful tool in understanding the molecular basis of neurobiology and neurodegeneration, as well as developing our current understanding of ageing [62,63]. These genetic approaches can be applied to study a specific pathogenic process, allowing for precise mutations to be generated, and with the use of balancer chromosomes, allows the maintenance of complex stocks with multiple mutations on a single chromosome to be generated and maintained, allowing for a powerful model for the pathogenic process of interest [60,63].

1.8 Aims of the study

Previous work conducted by Nathan Garnham[32] in the Sweeney lab investigated the roles of the AP-1 heterodimers, Fos and Jun, in the nervous system as a signaling pathway in neurons during oxidative stress. This study found that in Drosophila Punch was found bound to AP-1 in normoxic conditions, but not bound under conditions of oxidative stress. Punch is non-competitively inhibited by high levels of BH_4. Oxidation converts BH_4 to BH_2, decreasing the concentrations of BH_4 in the neurons. Subsequent studies showed that BH_4 induced binding of Punch to AP-1 and inhibition of AP-1 activity. High levels of ROS, potentially through oxidation of BH_4 reversed Punch binding to AP-1 and release of AP-1 activity. This project will follow on from this work by further investigating the role of Punch and AP-1 interaction and the movement and binding of the AP-1 heterodimers in the presence of oxidative stress in the nervous system of *Drosophila*. To further clarify both work in this project and the work previously conducted, we will manipulate the levels of BH_4 within the *Drosophila* system to further understand the impact of the Punch-AP-1 interaction and JNK signaling pathway in response to changing levels of ROS.

The specific aims of the study are:

- Determining the impact of Punch and AP-1 function on synapse growth when ROS levels change
- Manipulate the levels of BH_4 within *Drosophila* to further understand the impact of Punch function in the cellular response to ROS
- Understand the movement and binding of Punch to Fos and Jun when ROS levels change

Chapter 2. Materials and Methods

2.1 *Drosophila* husbandry and related techniques

2.1.1 *Drosophila* stocks

During the investigation, new *Drosophila* stocks were gathered from stocks already in the lab's repertoire and either used or crossed to generate new stocks. A full list of utilised stocks is shown in Table 2.1.

Table 2.1. List of *Drosophila* stocks used throughout this investigation [64]

Stocks	Chromosome	Description	Reference
Wild-Type			
W-	n/a	Wild-Type, White Eyes	Sweeney Lab Stock
GAL4 Stocks			
*Spin*GAL4/*TM6b*	Third	Spinster Promoter: Pre and Post Synaptic Driver	FBtp0016757
UAS Stocks			
UAS-*DHFR*	Third	Drives expression of DHFR	Sweeney Lab Stock[58]
UAS-Punch-HA	Second	Drives expression of Punch	Sweeney Lab Stock[58]
UAS-Punch-RNAi P(TRIP:HMS02399)	Second	RNAi to reduce Punch Activity	BDSC_41998
Mutants			
$Punch^{EY02616A}$/*CyO-GFP*	Second	Transgenic insertion (P(EPgy2)) disrupting Punch expression	BDSC_15576
$Punch^{R1}$/*CyO-GFP*	Second	In(2R)Pur1, spontaneous	BDSC_1002
Puc^{E69}/*TM6b*	Third	puckered LACZ reporter (P-element)	Kyoto 109029
Hiw^{ND9}/*Y*	First	Highwire null mutation	FBal0118195
Other Transgenes			
Jra-GFP.FLAG	Third	C-terminally GFP.FLAG tagged Jun isoforms A, B and C	BDSC_50755
Kay-GFP.FLAG	Second	C-terminally GFP.FLAG tagged kay isoforms A, B, D and F	BDSC_38657

2.1.2 *Drosophila* husbandry

Stocks were maintained within 25cm^3 plastic vials (Narrow Polystyrene vials; Flystuff) containing roughly 7ml of fly food, composing of 10g/l Agar (Agar, Pure powder; Acros Organics), 39.12g/l maize flour (Gluten-free organic maize flour), 37g/l Yeast (Pure Yeast, Lesaffre Human care; Lynside), 93.75g/l Sucrose (Sucrose, analytical; Fischer Scientific) and 6.75ml/l Propionic Acid (Acros Organics).

Experimental stocks were raised on instant food (Formula 4.24; Carolina Biological Supplies) containing 10% Ethanol-Yeast paste (inactivated) plus pharmacological agents when required. Inactivated yeast was prepared by mixing 20g of dried yeast (Dried active baking yeast; Allinson) with 100ml ddH_2O, forming a thin yeast paste. This was repeatedly boiled to inactivate the yeast and mixed to reduce the volume to a thick yeast paste, which was heated at 37^{o}C until dry, allowed to cool and mixed with 200ml of 10% ethanol (Fischer Scientific) to rehydrate before adding 60g of instant food to produce instant food with a final ethanol concentration of ~10%. Once fully saturated, roughly 3g of instant food was placed within a plastic vial, plugged with cotton wool (cotton balls for 25mm vials; Flystuff) to prevent flies escaping and allow the passage of air, and placed into a cold room at 4^{o}C to store until use. Pharmacological agents were made up in 10% ethanol and mixed with the dried yeast paste when required.

Stocks were maintained at 18^{o}C and transferred to new food every 4-5 weeks. Experimental crosses were all raised at 25^{o}C and transferred to new food every 3-4 days for as long as required. Fly selection and observation was performed whilst the flies were anesthetised, achieved via transferring flies to a porous pad connected to a compressed CO_2 gas cylinder (Dutscher Scientific, UK). Dissection microscopes (Stemi 2000 dissection microscopes; Zeiss) were used to view the flies.

2.1.3 Crossing

Crosses were performed using virgin females and males of the required genotype. Virgin females were selected either by observation of the meconium (first faecal matter observed as black spot in the abdomen of freshly emerged flies), if the wings were unexpanded or if the fly was known to be less than 8 hours old. Virgin females were kept separate from males for at least 3 days, ensuring no mating has occurred.

2.2 Immunohistochemistry and neuromuscular junction imaging

2.2.1 Third instar larval dissections and staining

Wandering 3rd instar larvae were selected, defined when they begin to exit the food and onto the sides of the vial. Their phenotypes checked to ensure correct sex based on the presence of gonadal imaginal discs and genotype based on GFP expression from balancer chromosomes and then dissected in Phosphate Buffered Saline (PBS) (Gibco) and fixed in 3.7% formaldehyde (Sigma) in PBS solution for 7 minutes. The larvae were pinned down by the anterior and posterior end in a droplet of PBS, cut laterally using scissors and their innards removed carefully. The muscle body wall was then pinned at each corner and the PBS replaced with 3.7% formaldehyde/PBS solution to fix the sample. After 7 minutes, the samples were unpinned and transferred into a 1.5ml Eppendorf tube containing PBS containing 0.05% Triton X-100 (PBST) and washed for up to 15 minutes. Once washed, the primary antibodies were added to stain the samples overnight on a nutator at 4°C. The samples were washed once more in PBST for up to 15 minutes before adding the secondary antibodies and left on a nutator at room temperature for 2 hours. After washing again, the samples were suspended in 70% glycerol/30% PBST solution at 4°C overnight. The dissections were then mounted on a microscope slide in mounting media (Vectashield) and a cover slip carefully placed on top and sealed with nail varnish. Once dried, the samples are stored out of direct light to prevent bleaching of the samples.

Table 2.2. List of antibodies used during this investigation

Primary Antibody	Strains	Conc	Host	Source
Anti-Horseradish-peroxidase-Cy3 (HRP-Cy3)	Neuronal Tissue	1:200	Goat	Jackson Laboratories (AB_2307391)
Anti-synaptotagmin (Anti-SYT91)	Synaptic Boutons	1:2000	Rabbit	Sweeney Lab
Anti-Punch182	GTP Cyclohydrolase 1/Punch	1:10000	Rat	Sweeney Lab
Anti-Punch183	GTP Cyclohydrolase 1/Punch	1:10000	Rat	Sweeney Lab
Anti-Tubulin	Tubulin	1:100000	Mouse	Sigma-Aldrich (T9026)

Secondary Antibody	Concentration	Source
Goat Anti-Rabbit-FITC	1:200	Jackson Laboratories (AB_2337972)
Anti- Rat Cy3	1:1000	Jackson Laboratories (AB_2338240)
Anti-Rat HRP	1:10000	Thermo Fisher Scientific (AB_228356)
Anti-Mouse HRP	1:10000	Thermo Fisher Scientific (AB_2533947)

2.2.2 Imaging and analysis of *Drosophila* NMJ

The quantification of the *Drosophila* NMJ through bouton count, branch number and synapse length began with antibody staining using anti-horseradish-peroxidase-Cy3 (HRP-Cy3) and anti-synaptotagmin/goat-anti-rabbit-FITC.

Using a Fluorescence microscope with CCD, the NMJ between muscles 6/7 at segment A3 were analysed and imaged. Each NMJ had its boutons counted using x63 objective and an image of the muscle was taken at x20 objective. The muscle surface area (MSA) was calculated for each NMJ using ImageJ and used to normalise the bouton and synapse length between genotypes. One Way ANOVA was conducted, ensuring data was normally distributed and there is homogeneity of variance between the datasets. Statistical analysis and graphs were conducted using R.

2.3 Measuring levels of oxidative stress

2.3.1 Amplex Red assay

To quantify the levels of ROS within Drosophila, an Amplex Red Assay was used, which quantifies the levels of H_2O_2 within the fly. For every ml of HL3 medium (128mM NaCl, 2mM KCl, 1.8mM $CaCl_2$-$2H_2O$, 4mM $MgCl_2$-$6H_2O$, 35.5mM Sucrose, 5mM HEPES, pH 7.1-7.2), 5µl Amplex Red reagent (50µM)(Invitrogen) were added and 10µl HRP (10u/ml) (Thermo Scientific, Pierce). For each individual male fly, 0.2ml volume of solution was used. The male flies were added to 1.5ml microcentrifuge tubes, quickly tapped and 0.2ml of reagent was added quickly. The fly was then pulverised in the reagent, vortexed and quickly centrifuged then left to incubate at room temperature for 90min or until colour change occured. Once colour change occured, the samples were vortexed and 80µl aliquoted into a 96 well plate wells, running two duplicates for each fly and two duplicates for just the Amplex Red reagent. The absorbance was measured using a microplate reader equipped for excitation in the range of 530-560nm. One Way ANOVA was conducted, ensuring data was normally distributed and there is homogeneity of variance between the datasets. Statistical analysis and graphs were conducted using R.

2.4 Imaging colocalisation of Punch and AP-1

2.4.1 Larval brain dissection and staining

Female 3rd instar larvae were collected and used for the analysis of the CNS. The larvae were torn in half in 3.7% formaldehyde in PBS and the anterior half turned inside out, exposing the CNS. The cuticle with the attached CNS was placed into an 1.5ml microcentrifuge tube containing 3.7% formaldehyde in PBS and left on a rocker for 30 minutes at room temperature. Once fixed, the formaldehyde was removed and cuticles washed 3 times in PBST containing 10% Methanol for a total of 30 minutes at room temperature. During the first wash, the cuticles were frozen at -80 briefly and thawed to increase the antibody permeability. The partial carcasses were then incubated in primary antibodies in PBST overnight at 4^{o}C, washed 3 times in PBST then incubated in secondary antibodies in PBST for 2 hours at room temperature, washed in PBST then transferred into 70% glycerol in PBS overnight, ready to be mounted and imaged.

2.4.2 Imaging and analysis of larval brains

To image the localisation of Punch and Jra/kayak, a Jra or kayak- FLAG-GFP female larvae was used and stained using anti-Punch 182/ Goat anti-Rat Cy3. Using a confocal Zeiss LSM 880 with Airyscan on an Axio Observer.Z1 invert, the ventral nerve cord was imaged at x20 / x40 magnification to view the localisation of Punch and Jra/kayak. The intensity of 3 cells from each condition were measured using ImageJ, by using plot profile option. The graphs that were produced for both Punch and Jra are combined to produce the figures for analysis, allowing for comparisons between the intensity of Punch/Jra though the nucleus of the cell.

2.5 Immunoblotting

2.5.1 Adult protein extraction

Flies were collected and snap frozen on dry ice in a 1.5ml microcentrifuge tube. The Eppendorf tube was then placed into a 50ml falcon tube with dry ice and vortexed at full power 2-3 times. The heads were separated and placed into a fresh microcentrifuge on dry ice. 1x Roche Complete Protease inhibitor tablet was dissolved in 7ml RIPA buffer on ice, which is used as a lysis buffer. The heads were ground with a pestle and placed on ice with 100-200µl of RIPA lysis buffer and left to incubate on ice for 30 min. Once incubated, the heads were spun at full speed for 10-15 mins at $4^{O}C$, supernatant removed and stored in a new tube ready for protein quantification.

2.5.2 Protein quantification

A 2mg/ml BSA serial dilution in a 96 well plate diluted in RIPA to give 10µl per well which was used as the standards for the protein quantification. The samples were diluted (1, 1:2 and 1:10) in RIPA lysis buffer and 10µl of each diluted sample was added to each well. 200µl of Bicinchoninic acid (BCA) working mix (1:50 of 2 components in it) was added to all samples and standards and left for 30-60 min at $37^{O}C$ until the colour developed from green to purple. When developed, the plate was left to cool at room temperature to stop the reaction. The plate was then inserted in a plate reader with BCA setting at 562 nm. The data from the plate reader was inputted to a template spreadsheet to calculate protein concentrations and amounts to load in the SDS-PAGE gel to ensure a protein concentration of 7.5µg/µl is loaded in each well.

2.5.3 Casting SDS-PAGE gels

The gel casting frame was assembled and placed onto a casting mount. The comb placed and a mark 1cm below the comb was marked using permanent marker. The resolving gel was mixed using fresh APS and TEMED, made up to required percentage gel for protein size (10% was used during this investigation (Supplementary Table S4)). The resolving gel was then pipetted into the plate up to the mark, then a layer of isopropanol was added to the top to remove bubbles. Once set, the isopropanol was removed and the stacking gel was made up and poured on top of the resolving gel. The comb was then placed perpendicularly to the surface of the gel and left to set.

2.5.4 Loading and running the gel

Laemmli buffer (4% 10% SDS, 20% Glycerol, 120nM Tris-Cl, 0.01% 1% Bromophenol Blue pH 6.8) with 2-mecaptoethanol was mixed with the samples to run at a ratio of 1:4 for 20µl of sample. The samples were heated to 70-90^{O}C for 10 min while the gel was placed into the tank and the central reservoir filled and the remainder of the tank filled with a running buffer. The tank was placed on ice to prevent overheating. The comb was gently removed and once samples were ready, 10µl loaded into each well using a fine pipette alongside a PageRuler™ Plus Prestained Protein Ladder (ThermoFisher Scientifics). The gel then ran at 100V until the dye front reached the end of the gel.

PVDF membrane was cut to the size of the gel, with care taken to wear gloves, 4 pieces of Whatman paper about the size of the cassette were also prepared. The Whatman paper and pads were soaked in a transfer buffer and one pad placed on each side of the cassette and 2 pieces of Whatman paper on each side. The gel was then briefly dipped into a transfer buffer and placed on the black side of the cassette. The PVDF was soaked in methanol for 30-60 sec and placed directly over the gel and the cassette closed and reopened. Everything was rolled gently using a roller and the cassette closed, locked and placed into the apparatus. The cassette was run at 100V for 2-3 hours.

Once run, the cassette was disassembled and washed in TBS-Tween (50mM Tris-Cl, 150mM NaCl, pH 7.6, 0.1% Tween 20 detergent) for 2x 5 min. The membrane then blocked in TBS Tween + 5% marvel milk for 1 hour at room temp. Primary antibody staining was then done in the blocking buffer at 4^{O}C overnight, washed in TBS-Tween at room temp before secondary antibodies in blocking buffer for 1 hour at room temp, then washed for final time in TBS-T.

2.5.5 Developing the immunoblot with chemiluminescence

Once the ECL™ Prime Western Blotting Detection Reagent (Cytiva) was made up by mixing Solution A and B in a 1:1 ratio, the washing buffer was removed from the membrane and immersed in chemiluminescence solution for ~30 seconds then dried using Whatman paper. The protein positive side of the membrane was placed facing down onto a sheet of clingfilm and the membrane wrapped and sealed into the clingfilm, placed into a radiography cassette and taken to the darkroom with infra-red light. An X-ray film was then placed over the membrane in the cassette and left for 30 sec, then placed in developer for 1 min, rinsed in water and placed into fix for 1 min. After rinsing again, the X-ray film was dried and viewed under red light. This procedure was repeated with different exposure times to generate an optimal image.

2.6 Bioinformatics

2.6.1 DIOPT analysis of ortholog genes

DIOPT (DRSC Integrative Ortholog Prediction Tool) identifies the orthologs of genes and proteins between different species. For this investigation, the *Drosophila* genes were inputted and the orthologs in the Human genome were identified. The highest score match was used during the investigation and the protein alignment showed similarity and identity percentages.

2.6.2 STRING analysis of protein-protein interaction networks

The protein name or accession number were used to find and generate the protein-protein interaction network using STRING. The minimum required interaction score was reduced to low confidence (0.150) and the interaction network was increased to show other proteins that interacted with the main proteins of this investigation, allowing for interactions with Punch, jra and kayak with lower confidence to be seen.

2.6.3 ENCODE identification of Fos and Jun genomic binding sites

ENCODE (Encyclopedia of DNA elements) is a large public database of DNA elements and ChiP-Seq datasets. The transcription factor of interest is searched for and ChiP-seq datasets that use the transcription factor as a target are shown. Within the file details contain the raw sequencing data, for which the bigWig and bed files, including control normalised signal, signal of unique reads and peaks, are downloaded. These files were opened and analysed in Integrative Genomics Viewer and the genes of interest were searched and analysed.

2.6.4 Statistical analysis

All statistical analysis was performed in R using a One-Way ANOVA test. Normal distribution was tested by conducting within R too. First a Q-Q plot was drawn to show correlation between samples and normal distribution, allowing us to identify points that do not fit normal distribution. Then a Shaprio-Wilk was conducted to test normality. If normality was not met, then points identified from the Q-Q plot were removed from the statistical analysis.

Chapter 3. Bioinformatic analysis of AP-1, *AP-1* responsive loci and their interactions

3.1 Bioinformatic analysis of putative *AP-1* responsive loci

Transcription factors including AP-1 are proteins that are involved in the initiation and regulation of the transcription of genes through specific binding to DNA sequences. These sites include promoter sequences, which recruit these factors and initiate transcription, and enhancers, which help target transcription factors to potentiate specific gene transcription. The Punch/AP-1 interaction has the potential to contribute to the regulation of AP-1 mediated transcription by Punch in a feedback loop whereby Punch expression is regulated by AP-1. GeneCards [65] states that the top transcription binding site in the GCH1 promoter is AP-1 according to the QIAGEN databases. In *Drosophila* Puckered (Puc) is a known AP-1 target which negatively feedbacks with JNK to repress AP-1 activity, which we believe may share similarities between AP-1 and Punch. Therefore, we used in silico analysis to confirm that GCH1 may be a putative transcriptional target of AP-1 within the mammalian system, and also investigate whether the *Drosophila* ortholog Punch there is evidence for transcriptional regulation of Punch/GCH1 by AP-1.

3.2 DIOPT analysis of orthologs used within this investigation

To begin the investigation, we began by confirming the *Drosophila* orthologs of the other genes of interest used throughout this project. A DRSC Integrative Ortholog Prediction Tool (DIOPT) analysis was first conducted to confirm the *Drosophila* orthologs and identify their alignment similarity. We used the human transcripts, for example Fos and Jun, to identify their closest orthologs in *Drosophila*. This confirmed that Punch was the best scoring ortholog of GCH1, kayak was best scoring ortholog of Fos and Jra was best scoring ortholog of Jun. MAPK8 and DUSP10 were also tested as they appeared to be the ortholog of the *Drosophila* AP-1 regulators basket and puckered respectively and would be used as positive controls in future bioinformatics and potential experiments. All DIOPT scores, ranking and alignment similarity scores are shown in Table 3.1.

Table 3.1. DIOPT analysis of ortholog genes

Human Gene	*Drosophila* Gene	DIOPT Score	Rank	Best Score	Alignment Similarity
Fos	kay	6	High	Yes	38%
Jun	Jra	11	High	Yes	47%
MAPK8	bsk	12.87	High	Yes	88%
GCH1	Pu	13.74	High	Yes	72%
DUSP10	Puc	7.8	High	Yes	44%

3.3 Promoter and enhancer analysis of *AP-1* responsive loci

Previous studies have shown that AP-1, specifically the Fos-Jun complex, play a central role in enhancer selection, together with cell type-specific transcription factors to select enhancer repertoires [66]. Therefore, we hypothesised that AP-1 may have implications in the initiation and promotion of *GCH1* transcription to gain insight into potential transcription feedback loops regulating GCH1 abundance, similar to the known feedback loop of AP-1 and Puc shown in Figure 3.1.

Using GeneCards, an integrated database of human genes that provides concise genomic related information, numerous promoters and enhancers within the GCH1 gene were identified containing transcription factor binding sites for a number of members of the Fos and Jun family shown in Table 3.2, with Gene Association Scores representing the degree of confidence based on numerous methods, such as transcription factor binding site score and proportion of supporting enhancer sources [67]. This may indicate that AP-1 plays a role in up-regulating the levels of GCH1 transcription to potentially further the production of BH_4 and folate production through interactions of these promoter/enhancers. MAPK8 and DUSP10 were also investigated as positive controls since they have been shown to be under AP-1 regulation [68–70], both showing numerous promoters and enhancers that contain Fos and Jun family member binding sites shown in Table 3.3 and 3.4.

Table 3.2. Promoter/Enhancer analysis of the *GCH1* locus in Humans (GeneCards)

GeneHancer ID	GH Type	Gene Association Score	Transcription Factor Binding Sites
GH14J054899	Promoter/Enhancer	617	FOS
GH14J054870	Enhancer	28.6	X
GH14J055113	Promoter/Enhancer	11	JUND, JUN, FOS, FOSL1
GH14J054818	Enhancer	16.7	JUND, JUN, FOS, FOSL1, FOSL2
GH14J055100	Enhancer	9.9	JUNB, JUND, FOS, FOSL1, FOSL2

Table 3.3. Promoter/Enhancer analysis of the *MAPK8* locus in Humans (GeneCards)

GeneHancer ID	GH Type	Gene Association Score	Transcription Factor Binding Sites
GH10J048305	Promoter/Enhancer	606.4	JUND, FOSL1
GH10J048386	Enhancer	20	JUND
GH10J048476	Enhancer	13.5	X
GH10J047401	Enhancer	12.7	JUND, FOS, JUN, JUNB
GH10J048333	Enhancer	24.3	FOS, JUND, FOSL2

Table 3.4. Promoter/Enhancer analysis of *DUSP10* locus in Humans (GeneCards)

GeneHancer ID	GH Type	Gene Association Score	Transcription Factor Binding Sites
GH01J221739	Promoter/Enhancer	628.1	FOS, JUND, JUN, FOSL1, JUNB
GH01J221706	Promoter/Enhancer	37	JUND, JUN, FOS, FOSL1, FOSL2, JUNB
GH01J221687	Enhancer	23	FOSL1, JUNB
GH01J221986	Enhancer	16.5	JUND, FOS, JUN, FOSL1, FOSL2, JUNB
GH01J221809	Enhancer	20	JUND, JUN

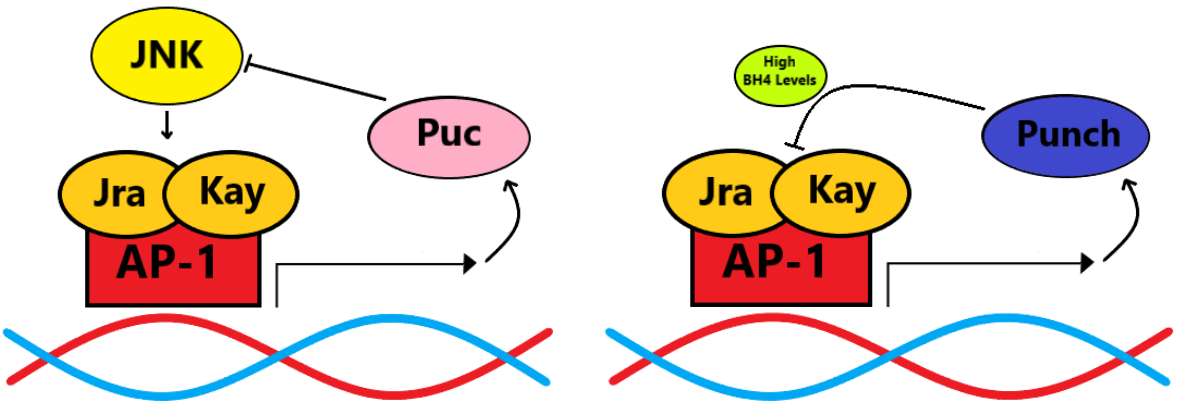

Figure 3.1. Interaction similarities between AP-1, JNK (MAPK8) and Puc (DUSP10) compared to AP-1 and Punch hypothesis

Schematic showing the regulation interaction between AP-1 by JNK and Puc and the hypothesised interaction between Punch and AP-1 in conditions of high BH_4. Phosphorylated JNK activates c-Jun leading to the formation of AP-1. Puc is transcribed by AP-1 and negatively feedbacks on JNK and inhibits its activity to stabilise AP-1 and reduce transcriptional activity through a negative feedback loop. We hypothesise that Punch is involved in a negative feedback loop with AP-1 in conditions of high BH_4 levels, leading to reduced transcription of Punch and therefore reducing the levels of BH_4.

3.4 Specific transcription factor binding sequence analysis

To further investigate the potential of AP-1 binding to the *GCH1* gene, analysis using Biogrid/LASAGNA, an integrated web tool for transcription factor binding site search and visualization, was conducted to identify specific binding sequences of c-Fos, c-Jun, AP-1 (Jun Family) and Fos-Jun heterodimer within the GCH1 gene. As shown in Table 3.5, all sequences containing a P-Value of below 0.05 were identified, along with their position and strand. There are numerous binding sites throughout all the Fos and Jun members and AP-1 complexes. The promoter/enhancers with the highest gene association score of 617 in GCH1 shows a transcription factor binding site specifically for Fos only, while the lower scores ranging from 11 to 9.9 show numerous Jun and Fos family member binding sites. These sites were located on the GCH1 gene in Figure 3.2, showing the majority of binding sites being present either before or on the first exon. This analysis was also conducted on MAPK8 and DUSP10 to act as positive controls within this bioinformatic analysis, which both showed numerous putative binding sites for both Fos and Jun in most, if not all promoter/enhancers listed.

Table 3.5. Biogrid/LASAGNA analysis of AP-1 binding sites in the *GCH1* Gene

Transcription Factor	Sequence	Position	Strand	P-Value
c-Fos	CGCGTCACGGC	356	-	0.0287
c-Fos	TCGCGTCAC	359	+	0.0353
c-Fos	TCGCGTCA	360	-	0.04835
c-Jun	AGTGTGATCTAAGCAG	472	+	0.0084
c-Jun	CTGCTTAGATCACA	474	-	0.024225
c-Jun	GTGTGATCTAAGCAG	473	+	0.03415
c-Jun	CTGCTTAGATCAC	475	-	0.0384
c-Jun	TGATCTAAGCAG	476	+	0.043675
AP1 (Jun Family)	TGCCTC	184	+	0.00625
AP1 (Jun Family)	TCACTGA	157	+	0.009975
AP1 (Jun Family)	TCAGTGAG	156	-	0.19825
AP1 (Jun Family)	TGCGTAC	490	+	0.02175
AP1 (Jun Family)	TGCCTG	43	-	0.022775
AP1 (Jun Family)	TTCCTAA	11	+	0.02345
AP1 (Jun Family)	TCCCTCC	262	+	0.024525
AP1 (Jun Family)	TCATTCC	204	+	0.02725
AP1 (Jun Family)	TGACGC	360	+	0.037825
AP1 (Jun Family)	TTTCTCA	153	+	0.042475
AP1 (Jun Family)	TAACTC	27	+	0.044925
AP1 (Jun Family)	TGGCTTA	22	+	0.4955
Jun/Fos Heterodimer	GAAAAGAGGCAGTC	181	-	0.00255
Jun/Fos Heterodimer	CCGATTAGGAACCA	8	-	0.0095
Jun/Fos Heterodimer	GGAATGAGCCCGAAC	197	-	0.01185
Jun/Fos Heterodimer	TCAGTGAGAAAGAC	150	-	0.0144
Jun/Fos Heterodimer	GGTTCGGCTCATTC	196	+	0.0159
Jun/Fos Heterodimer	AGAAAGACGCGGTC	144	-	0.022525
Jun/Fos Heterodimer	AGGCTGAGCCGCCG	402	+	0.02233
Jun/Fos Heterodimer	CCGGCGGCTCAGCC	403	-	0.026275
Jun/Fos Heterodimer	GCCGTGACGCGAGG	356	+	0.02705
Jun/Fos Heterodimer	CGACTGCCTCTTTT	180	+	0.02775
Jun/Fos Heterodimer	AAAAGGAGGCGCGG	423	+	0.0324
Jun/Fos Heterodimer	TTGGTTCCTAATCG	7	+	0.042025
Jun/Fos Heterodimer	CGTCTTTCTCACTG	149	+	0.04435

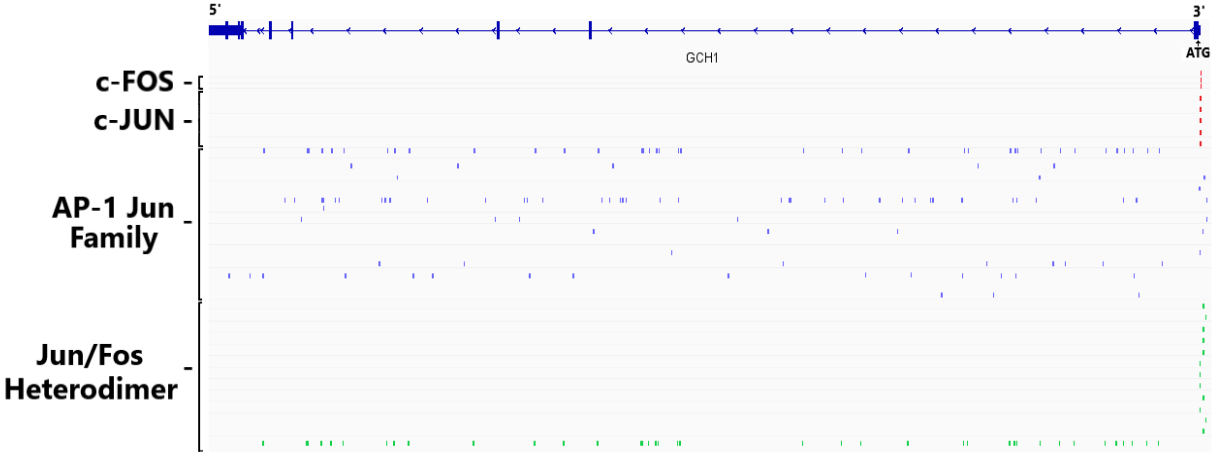

Figure 3.2. Identified locations of LASAGNA sequences within mammalian *GCH1* gene

The sequences identified within the LASAGNA analysis were located within the mammalian *GCH1* gene using Integrative Genomics Viewer. The sequences were searched and points marked below the *GCH1* gene. Some searches showed singular points, for example c-Fos and c-Jun sequences, while others showed numerous sequences throughout the gene.

3.5 Using STRING Analysis to define functional interactions between AP-1 and GCH1

The hypothesis of Punch/AP-1 interaction being part of a feedback loop where Punch, a product of AP-1 transcription, feeds back to regulate AP-1 activity was further explored by bioinformatic analyses of protein-protein interactions. A STRING analysis which looks into the functional protein association networks was conducted. This is a biological database of known and predictive protein-protein interactions. A score is given on the basis of known experimental evidence and predicted interaction for example. We inputed Punch, Jra, kayak and Puc and minimum required interaction score reduced to low (0.150) and extra proteins option added to the interaction map. The output obtained as shown in Figure 3.3, shows that there are known and predicted interactions between Punch and kay/Jra within the *Drosophila* system. Our positive control of Puc shows very clear interactions between numerous proteins including Jra, kay, bsk (MAPK8) and numerous others.

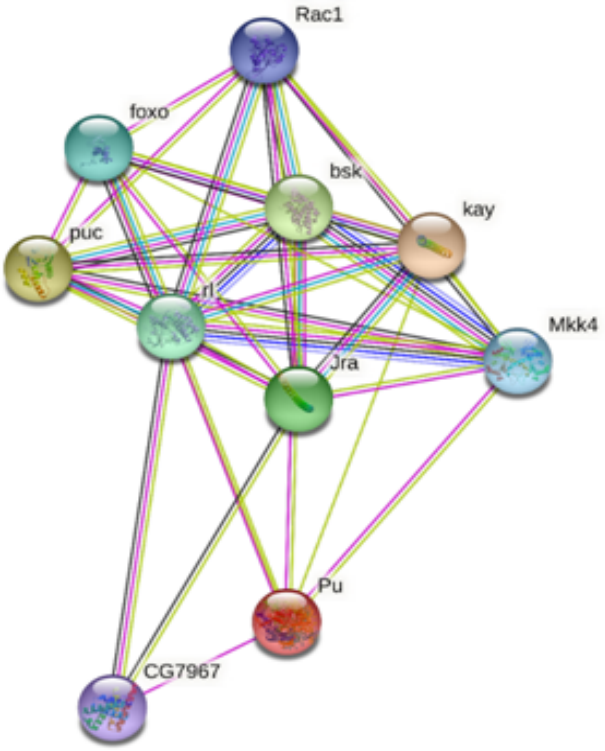

Figure 3.3. STRING analysis of Punch and AP-1 within the *Drosophila* interactome

The known and predicted protein-protein interactions were mapped using STRING, with low confidence (0.150) and with extra proteins added to form a bigger interaction web. This identified protein-protein interactions between Pu and Jra/kayak, implicating potential transcriptional regulation of Punch by AP-1. Puc was used as a positive control within this analysis. Line colours are evidence as follows. Red- Presence of Fusion. Green - Neighborhood. Blue - Cooccurrence. Purple - Experimental. Yellow - Textmining. Light Blue - Database. Black - Coexpression.

3.6 ENCODE analysis of Punch and Puc

To further investigate the potential interactions between Punch and AP-1 within the Drosophila system, we used ENCODE (Encyclopaedia of DNA Elements) to locate previous ChIP-Seq analysis of Jra and kay genomic binding. We investigated if transcriptional regulatory elements (TRE) sites were present in areas of both Jra and kay binding (implicating AP-1 binding) within *Punch* and our positive control *Puc*. ChIP-Seq is a method used to analyse the protein interactions with DNA, making it useful for identifying transcription factor binding sites within target genes. TRE (TPA-responsive elements) are conserved sequences that are recognised as the binding sites for AP-1. This consensus sequence has been defined as TGA(C/G)TCA, which even with a single nucleotide change can be recognised by AP-1. This sequence, with the singular nucleotide change variations, were located within the areas of Jra and Fos binding and shown with the arrows within Figure 3.4. Two arrows can be seen within the *Punch* gene, within an intron near the 3' end of the locus. The ChIP-Seq datasets used here were generated at different points of the *Drosophila* life cycle, one kay dataset in embryo, Jra dataset in 3rd instar larvae and final kay dataset in 3 day old fly, which may have an impact on our findings. There is also evidence that kay can homodimerize, while Jra can only dimerize with kay which may have further implications in AP-1 binding sites within these data sets [71]. A positive control of Puc was also conducted, clearly showing numerous TRE sites, within both introns and exons throughout the gene. The ChIP-Seq data on the *Puc* gene also shows numerous binding sites for Jra and kay throughout the entire gene, compared to Punch with very limited sites near the end of the gene.

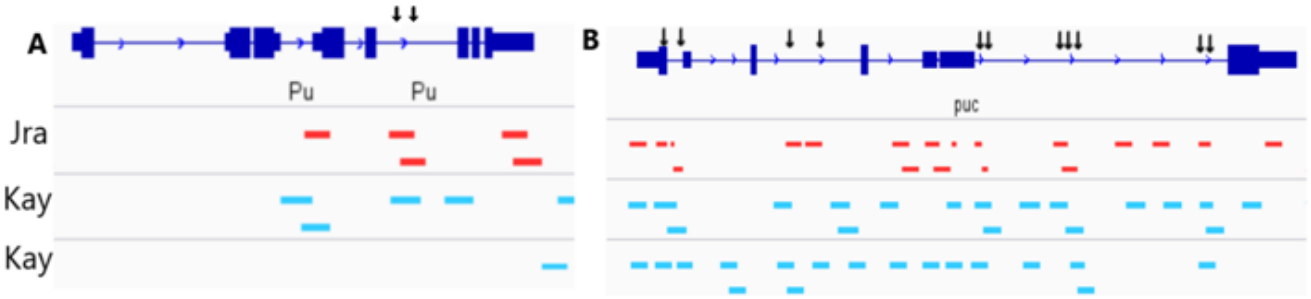

Figure 3.4. TRE sites potentially identified within Punch from ChIP-Seq data

ENCODE data analysed within Integrative Genomics Viewer using ChIP-Seq data for Jra and kayak. The overlap between jra and kayak binding to the GCH1 gene was identified and TRE sites with up to 1 nucleotide change were identified within these overlaps of binding and marked with arrows. These arrows potentially identify sites where AP-1 binds to the gene and regulate transcription. **A**) 2 potential sites were present within the *Punch* gene where jra and kayak both bind to the gene. **B**) Positive control of *Puc* locus was used, and shows numerous potential sites where AP-1 binds and regulates the gene.

3.7 Conclusions and future work

Building from our model hypothesis that AP-1 and Punch interact in conditions of excess BH_4 and/or physiological levels of oxidative stress, the potential for AP-1 to interact and promote the transcription of the *Punch* gene has been investigated. Within the Human system, the use of GeneCards to investigate promoter/enhancer transcription binding and Biogrid/LASAGNA to investigate specific sequence binding has both shown the potential of AP-1 activity on the *GCH1* gene. Numerous promoters and enhancers show the binding of a number of AP-1 family members, including Fos and Jun, which may implicate in the binding of AP-1 to these areas when oxidative stress levels increase, allowing for the promoted transcription of GTPCH1 and therefore the synthesis of BH_4 and folate. Studies have shown that AP-1 can be induced by signals to trigger a spectrum of cellular processes, therefore the theory that oxidative stress activates AP-1 and therefore leading to binding of the GCH1 gene would be plausible [68,69]. Biogrid/LASAGNA further builds upon this idea, identifying specific sequences within the *GCH1* gene that allow the binding of c-Fos, c-Jun and AP-1 complexes. This may potentially identify *GCH1* as another target of AP-1 transcription during the antioxidant response within the Human system. Further investigation could be conducted using previously known datasets, including ChIP-Seq data from ENCODE, to investigate the locations of Fos and Jun binding and potentially identify TRE sites within these areas, which may implicate further transcriptional regulation of the *GCH1* gene via AP-1. Laboratory work would have to be conducted to confirm this interaction. *In vivo* methods including ChIP-Seq could be conducted or *in vitro* approaches including SELEX (Systematic evolution of ligands by exponential enrichment) or DIP-chip (DNA immunoprecipitation with microarray detection) for example. This would allow for the interaction between the *GCH1* gene and AP-1 to be identified, and potentially tested under different conditions of stress with GTPCH1. It has been established that gene expression is significantly regulated by ROS-mediated signalling, therefore the interaction between the GCH1 and AP-1 could be regulated by ROS, allowing for the regulation of an antioxidant response along with the regulation of GCH1 and AP-1 activity [70].

Conducting bioinformatics within the *Drosophila* system is more difficult due to lack of known datasets in comparison to Human and Mouse models. A STRING analysis did show limited potential protein-protein interactions between Punch and kay/Jra, which may further aid our model hypothesis. Three ChIP-Seq datasets were used from ENCODE and showed 2 potential TRE sites within the *Punch* gene which may have implications in transcriptional regulation via AP-1. However, these were located within an intron close to the end of the gene. Experimental experiments must be conducted to confirm if these are indeed TRE sites and to confirm the binding of AP-1 to the *Punch* gene. The ChIP-Seq datasets were also taken from different age samples, as stated before, which may impact the results since transcriptional regulation changes throughout the development of an organism. Ideally, a kayak and Jra ChIP-Seq dataset from a *Drosophila* system at the same age, either 3rd instar larvae or 3 day old adult fly, would be preferred. Again, laboratory work would need to be conducted to confirm this hypothesis, either through *in vitro* or *in vivo* methods as stated previously.

Chapter 4. Investigating Punch-AP-1 interaction within *Drosophila* model

4.1 *Punch* alleles show varying levels of Punch protein

The potential interaction between the *Drosophila* ortholog of GCH1, Punch and the transcription factor AP-1 was previously identified by Nathan Garnham [32]. To initiate our investigation into the validity and function of this interaction, we wished to first of all confirm the efficacy of our reagents. We first wished to confirm the validity of both the *Punch* mutants and anti-Punch antibodies that were used in both this project and the previous investigation conducted by Nathan Garnham. A Western Blot was conducted on protein extracts from 1 day old adult heads from our *Punch* mutants along with a positive control (*Punch* over expression) and negative control (Punch knock down using Punch-RNAi). As shown in Figure 4.1, the levels of Punch are reduced within both of our *Punch* heterozygous mutants, which include $Pu^{EY2616A}$/+and Pu^{R1}/+, or in trans with each other. To confirm the validity of this experiment, our positive control shows roughly similar Punch levels to WT, while our negative control shows a clear decrease in Punch levels, confirming not only that both our *Punch* mutants reduce Punch function but that the anti-Punch antibody works as expected. The samples were quantified prior to loading using the BCA assay to ensure equal loading concentrations and anti-tubulin was quantified to confirm all loading was conducted equally throughout all our samples.

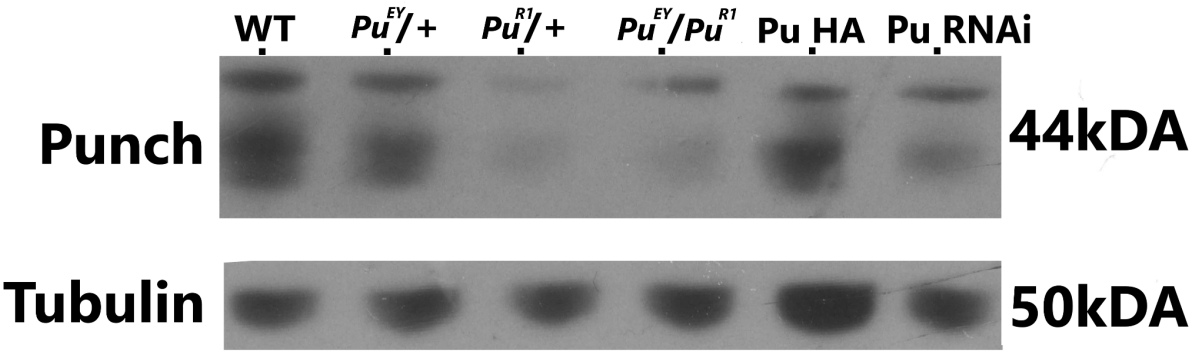

Figure 4.1 Punch protein levels are reduced within *Punch* allele mutants

Levels of Punch are shown to be reduced within Pu^{EY}/+and Pu^{R1}/+ adult heads, with Pu^{R1}/+ showing the lowest levels of the two mutants used within this investigation when using the anti-Punch antibody. A *spin-GAL4* cross was conducted with a positive control, UAS-Punch-HA (over expression), and a negative control, UAS-Punch-RNAi (knock down) to confirm the validity of the Western Blot. Tubulin was quantified to ensure roughly equal levels of loading were conducted for each sample. Molecular weights of bars are presented within the figure.

4.2 Reducing Punch levels releases AP-1 to drive synapse overgrowth under conditions of oxidative stress

Previous studies have shown that AP-1 is able to drive synapse overgrowth within the neuromuscular junction within 3rd instar larvae *Drosophila* [16,53,72]. Under conditions of oxidative stress, AP-1 can be a major mediator of synapse growth [31,73]. The data from Garnham [32] suggests Punch is capable through its binding of restraining AP-1 function. Therefore we hypothesised that manipulating the levels of Punch using the $Pu^{EY2616A}$ and Pu^{R1} mutants would release AP-1 and allow synapse overgrowth under conditions of stress. In keeping with Garnham, we induced oxidative stress in larvae by growing them in the presence of 10% ethanol, a mild oxidative stress. We also rescued oxidative stress induction via the feeding of the antioxidant Trolox, a Vitamin E analog. As shown in Figure 4.2, there is no change in synapse overgrowth within WT under 10% ethanol conditions, potentially due to the ability to deal with the slight increase in oxidative stress, while a significant increase in synapse overgrowth is shown to occur within these mutants under 10% ethanol conditions, with the increase of normalised bouton and branch number (Figure 4.2 A/B). This synapse overgrowth does not occur in within the *Punch* mutants in the absence of ethanol or when animals are treated with ethanol and 10mM Trolox, implicating this increase in synapse overgrowth is due to the oxidative stress caused by the 10% ethanol (Figure 4.2 C). However, although this synapse overgrowth is rescued, the regulation of ROS is not. To measure the levels of ROS within the *Drosophila* adults, an Amplex Red assay was used, which measures the levels of H_2O_2 within the adult heads. When grown in food without ethanol we see a slight significant increase in ROS in both *Punch* mutants, and a further significant increase within 10% Ethanol conditions (Figure 4.2 D). However, we were unable to entirely rescue this ROS increase using 10mM Trolox. Trolox feeding was only able to rescue ROS levels in the Pu^{R1}/+ conditions.

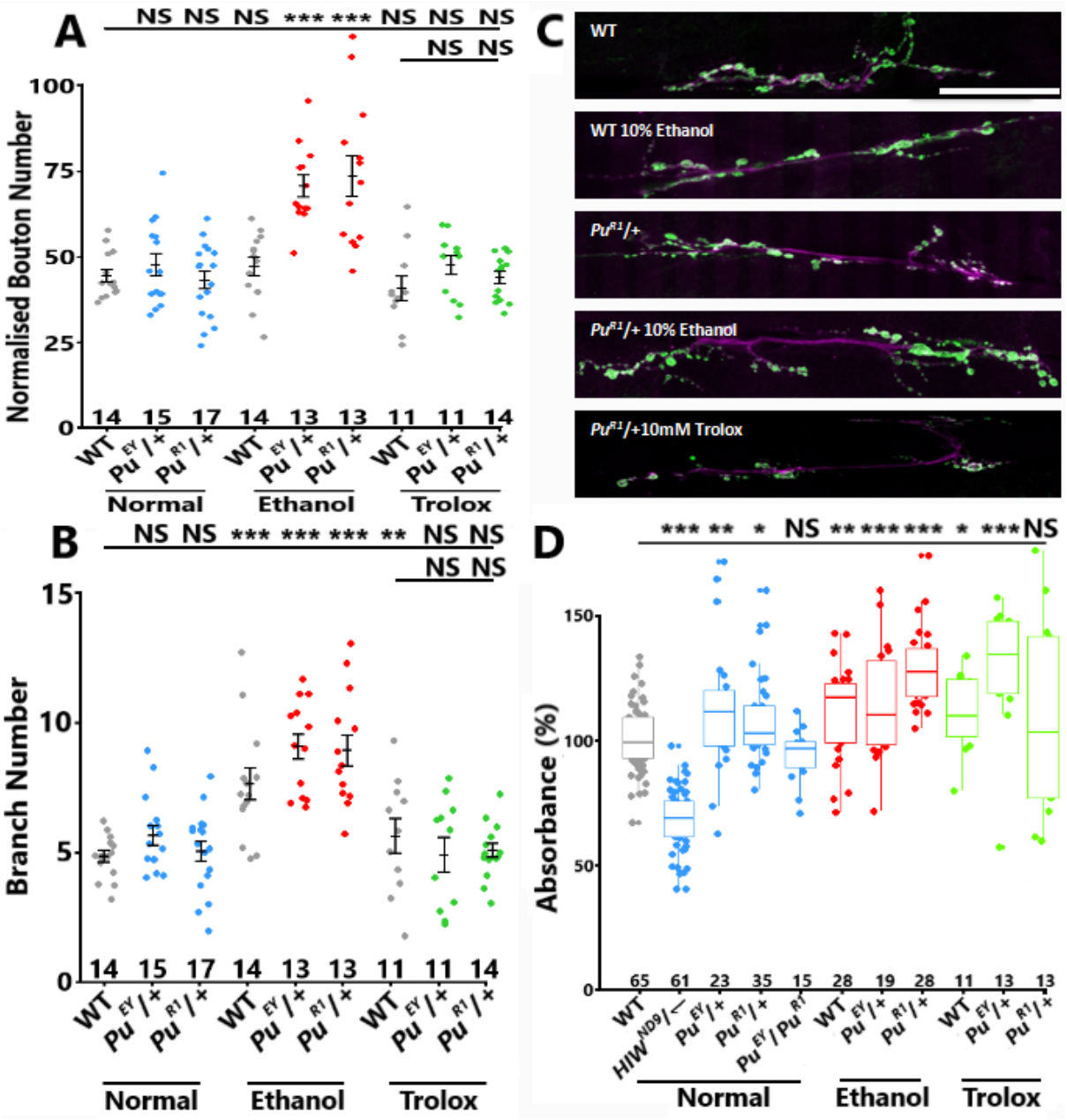

Figure 4.2. *Punch* mutants release AP-1, driving synaptic overgrowth under conditions of low oxidative stress

Levels of Punch were modified through the use of the Pu^{EY}/+ and Pu^{R1}/+ heterozygous mutants. **A/B**) Neuromuscular Junction Analysis (NMJ) was conducted on 3rd instar larvae, and normalised to WT. *Punch* mutants show an increase in synapse overgrowth through increased bouton and branch number in conditions of 10% ethanol, which can be rescued with 10mM Trolox. **C**) Confocal images of NMJs from specimens using HRP-CY3 (magenta) and anti-synaptotagmin tagged FITC (green). Scale bar – 50 microns. **D**) Amplex Red assay conducted on up to 1 day old flies and absorbance normalised to WT. Shows increased ROS levels present within *Punch* mutant flies on both normal and 10% ethanol food. One-way ANOVA was conducted for a statistical test. *** P< = 0.001, ** <=0.01, * <=0.05.

4.3 Increasing conditions of oxidative stress do not drive further synapse overgrowth in *Punch* mutants

Since showing that low oxidative stress conditions lead to a significant increase in synapse overgrowth and ROS levels in the *Punch* heterozygous mutants, we next wanted to test if further increasing ROS levels in high oxidative stress conditions, using 10mM Dethyl maleate (DEM), would further increase synapse overgrowth and ROS levels. DEM acts to deplete the cellular anti-oxidant glutathione [55]. As shown in Figure 4.3, we see that further increasing oxidative stress does not further drive synapse overgrowth, specifically within bouton count (Figure 4.3 A). There is a slight increase in branch number, which can also be seen within the confocal images in the strong oxidative stress conditions (Figure 4.3 B/C). The 10mM DEM treatment confocal image was previously taken with faulty synaptotagmin antibodies, and with lack of time was unable to produce an image containing both synaptotagmin and anti-HRP staining. This data suggests that the synapse overgrowth reaches a maximum at low oxidative stress conditions, with further oxidative stress barely impacting the increase in synaptic overgrowth. This can be again rescued with feeding of the anti-oxidant Trolox. However, we observed potential issues with the measurement of ROS levels using the Amplex Red Assay (Figure 4.3 D). In high oxidative stress conditions, we see no significant change in ROS levels between WT control with and without DEM. This may be an issue with the DEM-treated food and lack of repeats due to time constraints. The Trolox rescue of DEM-treated food seems to have rescued the ROS levels, which supports that the previous figures using Trolox-treated food rescued synaptic growth, but did not rescue levels of ROS in tissues under these conditions.

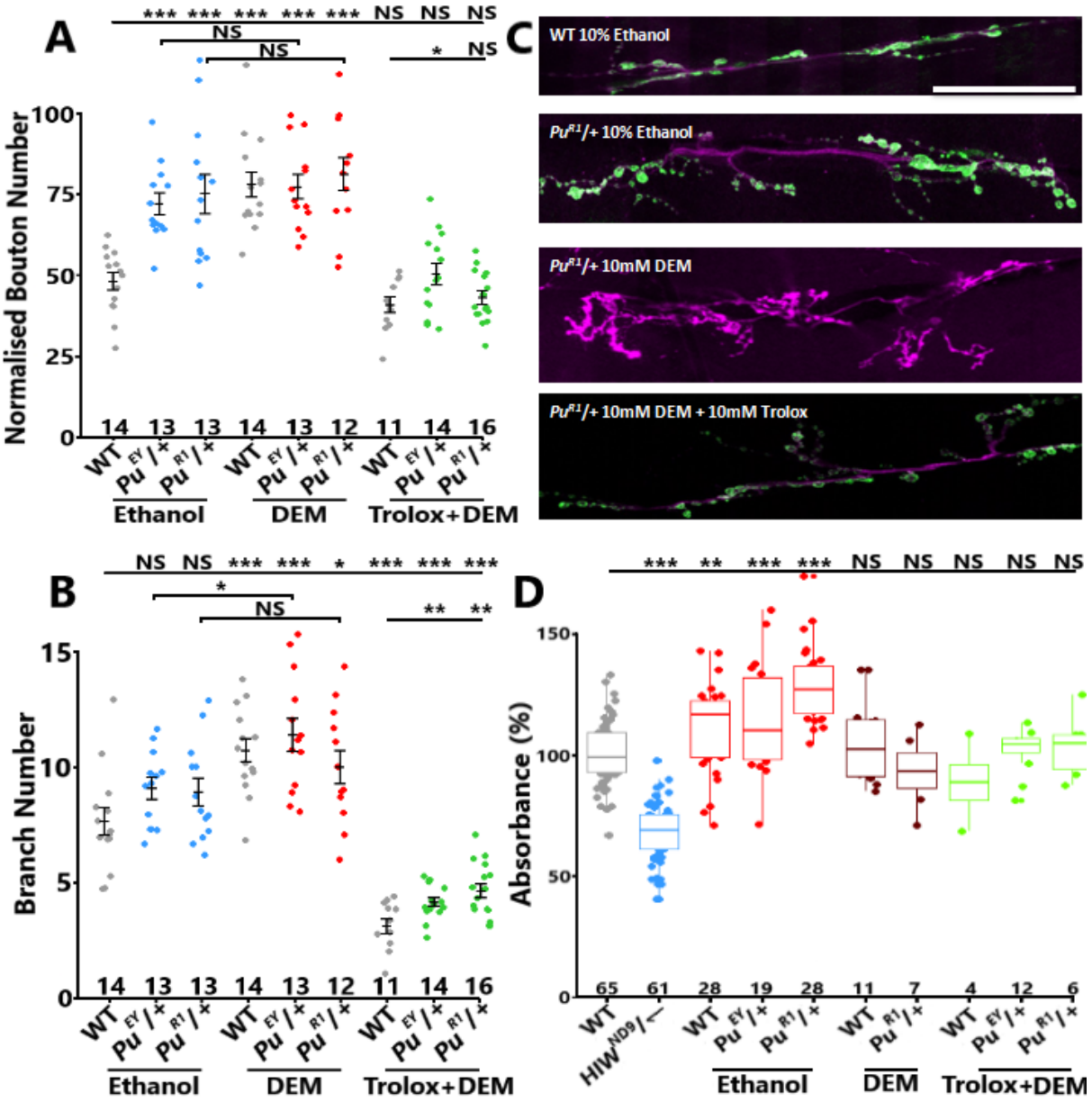

Figure 4.3. Increasing ROS levels does not drive further synapse overgrowth in *Punch* heterozygous mutants

Synapse overgrowth was investigated further using 10mM DEM feeding as well as testing the rescue of synapse overgrowth caused by DEM with 10mM Trolox. **A/B**) NMJ was normalised to WT on 10% ethanol. Further increasing ROS levels from 10% ethanol to 10mM DEM does not further drive synapse overgrowth implicating 10% ethanol drives maximum AP-1 transcription. 10mM DEM conditions can also be rescued with 10mM Trolox. **C**) Confocal images of NMJs from specimens using HRP-CY3 (magenta) and anti-synaptotagmin tagged FITC (green). Scale bar – 50 microns. **D**) Amplex Red assay with 10mM DEM food and Trolox Treatment. The results show reduced ROS within DEM food, which may be caused by issues with repeats and DEM food. However, the Trolox and DEM food rescues ROS levels back to WT level. One-way ANOVA was conducted for a statistical test. *** P< = 0.001, ** <=0.01, * <=0.05.

4.4 Raising BH_4 levels rescues synaptic overgrowth but not ROS levels when Punch levels are reduced

Since our previous findings have shown that manipulating the levels of Punch through $Pu^{EY2616A}$ and Pu^{R1} alleles leads to synaptic overgrowth, the next steps were to manipulate the levels of BH_4, the third component in our model hypothesis. Previous work conducted by Nathan Garnham showed that in excess of BH_4, Punch protein could be seen to interact with Kayak or Jra when levels of BH_4 were high. Therefore, we introduced increased levels of Dihydrofolate Reductase (DHFR) using a UAS-DHFR transgene in the *Punch* mutant background using the *spin*GAL4 line. *spin*GAL4 drives expression in motor neurons and muscles with a lower level of expression in glia [74]. This allowed for the over expression of DHFR to potentially reconstitute BH_4 levels from BH_2. As shown in Figure 4.4, this increase in BH_4 leads to the rescue of synapse overgrowth in both *Punch* heterozygous mutants in low and high oxidative stress conditions (Figure 4.4 A/B). The increase in BH_4 levels potentially allow the Punch and AP-1 to bind; preventing AP-1 transcription within the nucleus and therefore rescuing synapse overgrowth in every condition we used (Figure 4.4 C). However, this may also impact the ability for AP-1 to regulate ROS within these NMJs. We conducted an Amplex Red assay to investigate if the levels of ROS were also being rescued within these rescue flies. In normal conditions, we see an increase in ROS levels, similar to the *Punch* mutants alone and again in the low oxidative stress conditions, showing no rescue to ROS levels due to the increased BH_4 levels (Figure 4.4 D). A DHFR expression alone control was tested to see if this ROS increase was occurring only due to this over-expression, to which we see normal wild-type levels for these flies.

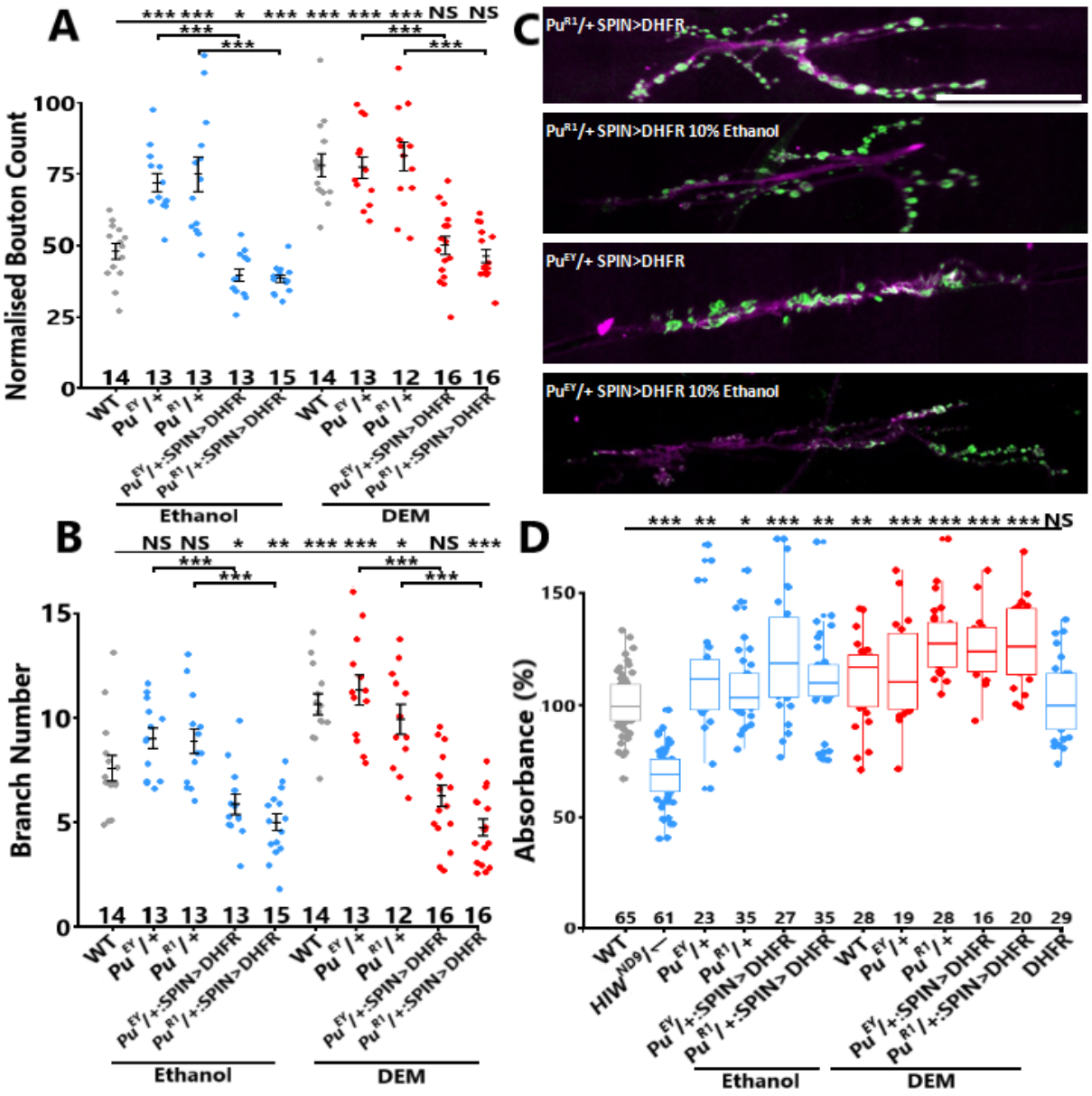

Figure 4.4. Over expression of *DHFR* rescues synaptic overgrowth but not ROS levels within *Punch* mutants under conditions of stress

The over expression of Dihydrofolate Reductase (DHFR) using spinGAL4-UAS system was conducted in order to increase the levels of BH_4 within the *Punch* mutants. **A/B**) NMJ was normalised to WT on 10% ethanol. Within the 3rd instar larvae *Punch* mutants, manipulating the levels of BH_4 rescued the synapse overgrowth, both normalised bouton and branch numbers. This not only rescued the synapse overgrowth back to wild type levels at 10% ethanol conditions, but also at 10mM DEM conditions. **C**) Confocal images of NMJs from specimens stained with HRP-CY3 (magenta) and anti-synaptotagmin tagged FITC (green). Scale bar – 50 microns. **D**) Amplex Red assay was conducted on the DHFR rescue flies. In both normal and 10% ethanol conditions, the *Punch* mutants with *DHFR* over expression continue to show increased ROS levels in both normal conditions and 10% ethanol, implicating the increase in BH_4 does not reduce levels of ROS, only rescues synaptic overgrowth. One-way ANOVA was conducted for a statistical test. *** P< = 0.001, ** <=0.01, * <=0.05.

4.5 Raising BH_4 levels rescues synaptic overgrowth within *hiw* mutants

Highwire (*hiw*) is a conserved protein which is involved in restraining synaptic growth and promotion of synaptic transmission within the *Drosophila* NMJ [75]. Mutations in this gene therefore lead to synaptic overgrowth due to an up regulation of MAP kinase signaling [72,76], while in zebrafish a strongly reduced level of BH_4 and increased level of BH_2 is observed [72,76]. Previous work to this investigation showed that overexpressing *Punch* rescued the synaptic overgrowth caused by mutations within *hiw* [32]. Therefore we introduced either Punch or DHFR using the *nSyb-GAL4* construct to investigate if we could rescue the effects of *hiw* on synapse overgrowth by recovering the levels of BH_4 using these genes. As shown in Figure 4.5 A/B/D, a clear drop in synapse overgrowth, in either bouton count, branch number or synapse length was observed in *Pu* heterozygous mutants with both the *Punch* and *DHFR* overexpression in background, indicating that the dysregulated AP-1 transcriptional output caused by the *hiw* mutation can be repressed through either increasing levels of Punch or BH_4. Even though a significant drop is seen in synapse overgrowth between the *hiw* mutant and the Punch/DHFR rescue (Figure 4.5 C), this was not fully rescued back down to WT levels. Further investigation into the levels of BH_4 within the *hiw* mutant and the rescues would allow us to identify if rescuing using Punch or DHFR recovers BH_4 levels and therefore reduces synaptic overgrowth through the binding of Punch/AP-1/BH_4 and therefore the inhibition of AP-1 activity.

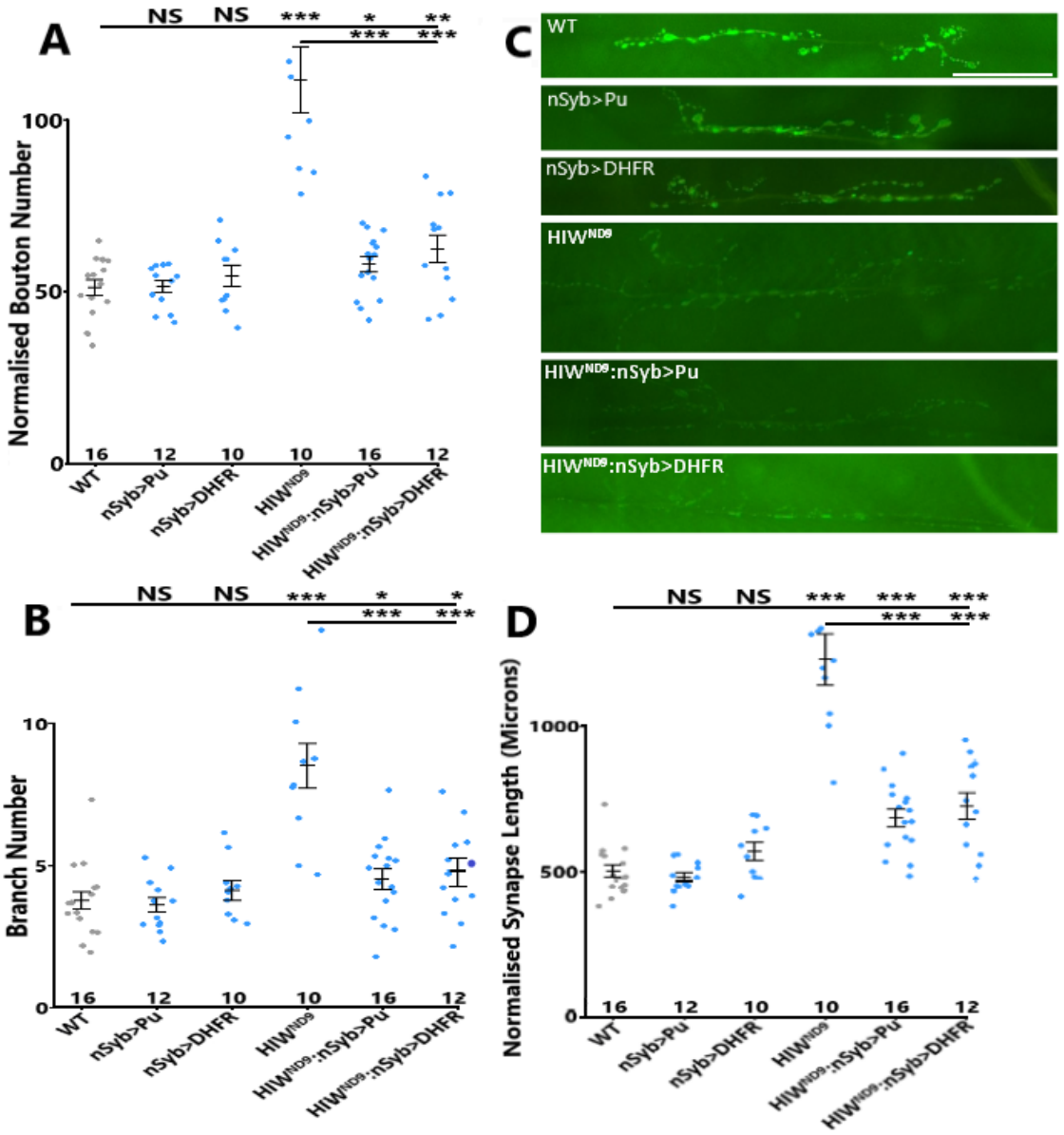

FIgure 4.5. Overexpression of *Punch* or *DHFR* rescues synaptic overgrowth caused by AP-1 dysregulation in *hiw* mutants

Overexpression of Punch or DHFR was conducted using nSyb-GAL4-UAS system to investigate if changes in Punch and BH_4 levels would counter the synaptic overgrowth caused by the dysregulation of AP-1 within *hiw*^{ND9} mutants. **A/B/D)** Synaptic overgrowth was measured through bouton counts, branch number and synapse length within the NMJ. Both bouton counts and synapse length were normalised to WT. The synapse overgrowth present in *hiw*^{ND9} mutants is significantly reduced through overexpression of Punch or DHFR. **C)** Epifluorescence images of NMJs from specimens using anti-synaptotagmin tagged FITC (green). Due to time limitations, confocal images were not conducted. One-way ANOVA was conducted for a statistical test. *** P< = 0.001, ** <=0.01, * <=0.05.

4.6 Colocalisation of Punch and Jra within *Drosophila* larval ventral nerve cord in normoxia and Dissociation in conditions of oxidative stress

Following on from our work and work conducted by Nathan Garnham, we next wanted to confirm if Punch and AP-1 colocalise within the larvae brain under normal conditions. Once dissected and imaged, we can clearly see a colocalisation of Jra (green) and Punch (magenta) within a cluster of cells in the ventral nerve cord of the 3rd instar larvae. This colocalisation seems to be occurring in only these clusters of 8 cells. These cells are potentially motor neurons which we attempted to confirm using either anti-EVE antibody or OK6-gal4, UAS-m-RFP gene. These experiments were however unsuccessful due to defective reagents. Jra-FLAG-GFP and Punch also seem to colocalise within the nucleus of these cells, with very limited Punch in the cytoplasm, potentially indicating most of the AP-1 and Punch are binding during normal, physiological levels of ROS within the nucleus and restraining AP-1 function in there. Confirmation that this was occurring specifically within the motor neurons and in the nucleus was unfortunately not possible due to lack of time.

Once we had identified that a possible colocalisation of Punch and Jra does occur within the ventral nerve cord in normal physiological conditions, we next wanted to identify if raising the ROS levels via 10mM DEM treatment would cause the dissociation of these proteins as hypothesised. As shown in Figure 4.6, we can see a reduction in colocalisation of Punch and Jra within the nuclei of the same cluster of cells. Punch also seems to be localising around the nucleus rather than within, potentially showing that Punch has dissociated from Jra and moved out of the nucleus. In this location it may act to allow the production of BH_4 and folate. A graphical representation of the intensity (Figure 4.7) of identified nuclei shown in Figure 4.6, which maps the intensity from one side of the cell to the other, further potentially shows this envelopment of Punch around the nucleus rather than localisation within the nucleus, with the Jra being more spread out in DEM conditions in comparison to similar shaped peaks in normoxia conditions. This may indicate that higher levels of ROS leads to the dissociation of Punch and Jra within the *Drosophila* larval brain system. Further repeats are required to quantify this colocalisation and dissociation, since only 3 cells per group have been studied, along with an internal control and identification of motor neurons specifically to confirm our theory.

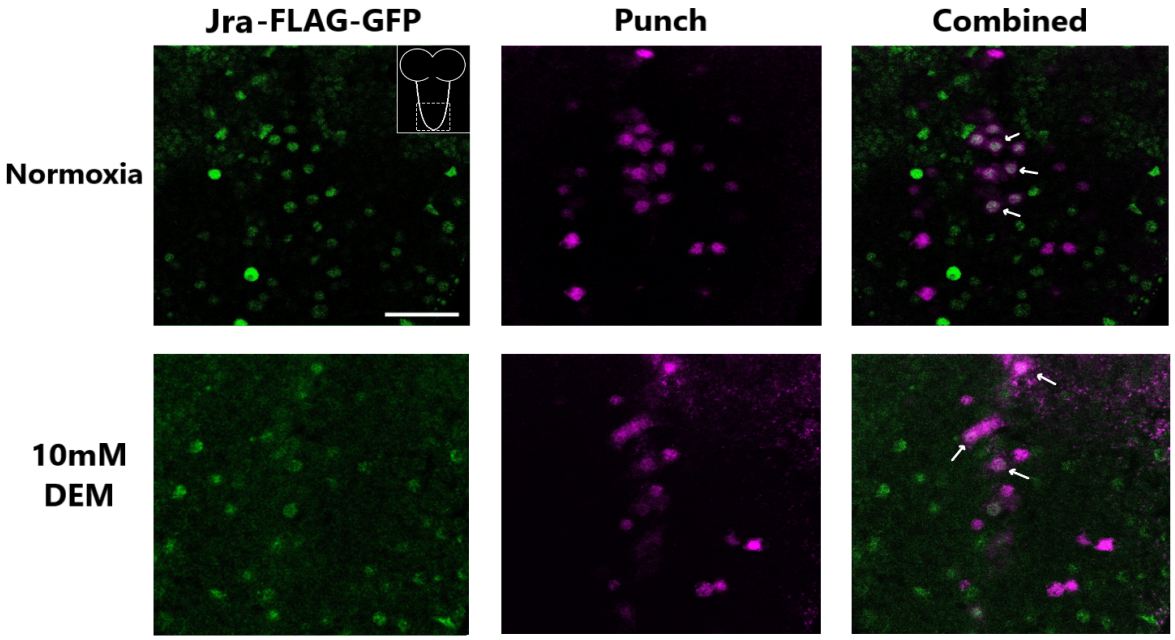

Figure 4.6. Punch and Jra colocalise within *Drosophila* larval ventral nerve cord in physiological ROS levels and dissociate in conditions of ROS

We probed the ventral nerve cord (VNC) of larvae for the colocalisation of Jra (green) and Punch (magenta). We identified a cluster of cells, potentially the motor neurons where Punch and Jra are both enriched. This colocalisation seems to occur within the nucleus of these cells, as shown by the lack of Punch around the cells and high concentration of colocalisation within. In conditions of 10mM DEM, we see the dissipation of Punch relative to Jra in these cells, potentially with Punch leaving the nucleus, however this requires quantifying. Arrows indicate cells used in analysis in Figure 4.7. Scale bar – 30 microns

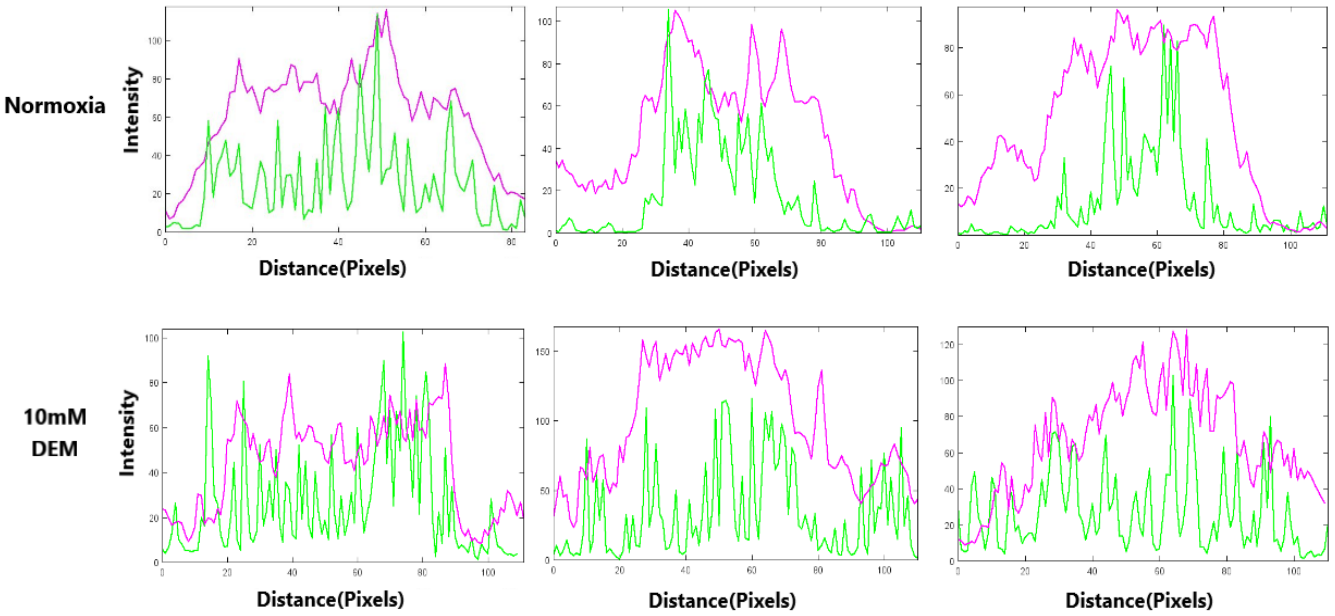

Figure 4.7. Changes in intensity of Jra in DEM conditions in comparison to conditions of normoxia

Intensity graphs were produced in ImageJ by measuring intensity of both Jra (Green) and Punch (Magenta) through the different cells within the larvae brain highlighted in Figure 4.6 (n=3). In normoxia conditions, the Punch and Jra intensities are similar in shape, implicating colocalisation within the nucleus of these cells. In 10mM DEM conditions, we see a different, flatter curve for Jra, which may imply dissociation of Jra and Punch. Punch levels also seem to be more dispersed too in comparison to normoxia conditions, however more cells must be studied to confirm this.

4.7 Conclusions and future work

We hypothesised that Punch and AP-1 functionally interact and bind together in conditions of normoxia and excess BH_4. To address this regulation of AP-1, we examined NMJ synaptic growth in *Drosophila* larvae, a process that is known to be AP-1 dependent [28,53,72].

The NMJ analysis supported the previous findings conducted within the Sweeney Lab [32]. It has been previously demonstrated that oxidative stress can induce NMJ overgrowth via a JNK/AP-1 dependent mechanism [31,73]. We found that in conditions of 10% ethanol, a mild oxidative stress, there is a significant increase in synapse overgrowth, both in bouton count and branch number, in both Pu^{EY}/+ and Pu^{R1}/+ heterozygous mutants, but not in wildtype animals. Treatment with an antioxidant rescues this overgrowth, confirming this overgrowth is indeed caused by the oxidative stress. We then examined synaptic overgrowth under a stronger oxidative stress challenge testing the Pu^{EY}/+ and Pu^{R1}/+ mutant responses to 10mM DEM conditions (Figure 4.2 and 4.3 respectively). Under strong oxidative stress challenge, the wildtype Pu^{EY}/+ and Pu^{R1}/+ mutant synapses were overgrown and this overgrowth could be rescued to non-treatment levels of growth. The overgrowth observed in the strong oxidative stress conditions was similar to that of the mild stress conditions.

This analysis builds a picture of *Punch* heterozygous mutations, where a reduced level of Punch protein is expected (Figure 4.1) leading to a reduced restraint on AP-1 when ROS is increased. Measurements of ROS levels (Figure 4.2D) show an increase within Pu^{EY}/+ and Pu^{R1}/+ mutants even in normal conditions, suggesting a reduced redox regulation within these flies. Unfortunately, due to issues with Trolox and DEM food treatments as well as lack of time for repeats, we were unable to complete sections of the Assay in Figure 4.2 and 4.3.

To test if upregulation of BH_4 by overexpression of *DHFR* could accentuate the AP-1 repressing function of AP-1, we attempted to rescue the synapse overgrowths within the Pu^{EY}/+ and Pu^{R1}/+ mutants under oxidative stress. DHFR converts BH_2 (the oxidised form of BH_4) to BH_4. Expression of DHFR in the Pu^{EY}/+ and Pu^{R1}/+ backgrounds while treating with mild or strong oxidative stress rescued synaptic overgrowth This rescue further builds on the hypothesis that excess BH_4 is required to allow the interaction of Punch and AP-1 to occur. This AP-1 repression is also seen in the *hiw* rescues in Figure 4.5, showing both the rescue through overexpression of *Punch* and *DHFR*. However, even though the *DHFR* overexpression leads to the rescue of synapse overgrowth, it does not appear to rescue the levels of ROS within *Punch* mutants. As shown by measuring ROS levels in these animals in Figure 4.4, these flies still hold a ROS burden similar to the *Punch* mutants, showing the complex regulation required between AP-1, Punch and BH_4 that is needed for redox regulation.

A potential *in vivo* association between Punch and AP-1 can be seen within our colocalisation experiments within the *Drosophila* larval ventral nerve cord immunohistochemistry. Figure 4.6 clearly shows the colocalisation of Punch and AP-1 within a selection of cells, which we predict are the motor neurons, specifically within the nucleus. This data does fall into our model hypothesis and also shows that this interaction may potentially occur within the nucleus of the cell. Previous studies using cell fractionation showed that GCH1 is present within the cytoplasm and nucleus when GCH1 is ectopically expressed [77]. When conducting the colocalisation experiment in conditions of high oxidative stress (Figure 4.6), we see a potential dissociation of Punch and AP-1 within the system (Figure 4.7), which fits with our model that in conditions of stress the interaction dissociates, allowing AP-1 to drive an antioxidant response. Punch immunoreactivity also seems to move out of the nucleus and potentially into the cytoplasm to produce BH_4. To further add to these findings, confirmation of which cells this colocalisation is taking place through either successful use of anti-Eve antibody or OK6-gal4-RFP gene to allow the visualisation of the motor neurons would be optimal. Confirmation on the location of this colocalisation within the nucleus would also be beneficial to this data, either through use of antinuclear antibodies or nuclear RFP markers.

Chapter 5. Discussion

5.1 A novel redox regulating interaction between Punch and AP-1

Throughout this project and the previous investigation conducted by Nathan Garnham [32], the potential for a redox-regulating interaction between Punch and AP-1 has been thoroughly investigated. Previous work described an interaction between Punch, Jra and kayak in conditions of excess BH_4, indicating not only the importance of BH_4 in this novel interaction but also the negative feedback loop that occurs. Under conditions of ROS, BH_4 would potentially be oxidised and AP-1 and Punch dissociate, leading to an antioxidant response by AP-1 and the production of BH_4 by Punch. Once ROS levels return to normal physiological levels, the excess concentration of BH_4 not only inhibits Punch through direct interaction within the *Drosophila* system but also promotes the association of Punch and AP-1. We potentially observe this interaction within the colocalisation experiment conducted within Figure 4.6 and 4.7, with Jra and Punch association occurring in normal conditions within the nucleus, which previous studies have shown an ectopically expressed GTPCH1 being present within both the nucleus and cytoplasm, as well as the membrane and mitochondria [77]. Under strong oxidative stress, we hypothesise that the dissociation and movement of Punch from the nucleus into the surrounding cytoplasm, which would presumably allow for the synthesis of BH_4. A Size Exclusion Chromatography experiment is currently being tested to confirm the interaction between recombinant AP-1 and Punch in either conditions of excess BH_4 or not within *In Vitro* conditions.

This novel interaction may be an important mechanism within neurons to detect and regulate the levels of ROS to prevent the damage of these highly sensitive cells. This interaction between AP-1 and Punch would be regulated by the levels of BH_4, which readily oxidise in the presence of ROS. Levels of excess BH_4 inhibit Punch and cause this association, preventing the production of further BH_4 and AP-1 transcription through this negative feedback loop. However, when these levels drop due to the presence of ROS, this interaction breaks, allowing an antioxidant response to occur and for levels of BH_4 to be replenished, allowing for a highly regulated antioxidant response to occur. We have shown that manipulating the levels of BH_4 through the use of *DHFR* overexpression reduces the activity of AP-1 within *Punch* mutants, however due to the imbalance of BH_4 levels, we see a dysregulated response to ROS levels, shown in Figure 3.8D. These results along with the previous NMJ analysis in Figure 4.2 and 4.4 show that the levels of both Punch and BH_4 must be carefully controlled to allow an regulated antioxidant response to occur. Our bioinformatics potentially show that Punch is a target of AP-1 (Figure 3.2 and Table 3.2),

which may imply that during the dissociation of AP-1 and Punch, AP-1 interacts with either the promoter/enhancers in the *Punch* gene, allowing the synthesis of further Punch. This further feeds into this hypothesis of the highly regulated interactions between Punch, AP-1 and BH_4, where impacting the levels of any protein in this regulatory association impacts this interaction and thus antioxidant response. This interaction may not be limited to these 3 proteins, as previous studies have shown that tyrosine hydroxylase (TH) interacts with GTPCH1 to prevent BH_4 inhibition and that administration of BH_4 could not fully restore the activity of TH if the GTPCH1 was mutated within the *Drosophila* system [49], further showing the delicate balance required between AP-1, Punch and BH_4.

5.2 Further implications of the Punch-BH_4-AP-1 interaction

Our data supports the finding of a novel interaction between AP-1, Punch and BH_4 in redox regulation. Our data further examines and uncovers functional consequences of this interaction Punch is most notably known as the first-rate limiting step in the synthesis of BH_4, however previous studies have identified up to 29 proteins which interact with GCH1 within the mammalian system [77]. These proteins ranged from kinases including the Death-associated protein kinase 3 and transcription factors such as interferon regulatory factor 1. This study suggested that the interactions between GCH1 and signal transduction molecules may be responsible for regulating GCH1 or allow GCH1 to serve as a signaling molecule. Our data potentially implicates GCH1 within the regulation of ROS, but also additional interaction data suggests roles in cell cycle regulation, cell proliferation and apoptosis, making the regulation of this protein highly important throughout the cell [78]. The mutation or dysfunction of GTPCH1 therefore has implications for numerous diseases and disorders. Mutations in GTPCH1 and therefore the reduced synthesis of BH_4 has been shown to cause the dysfunction of the nigrostriatal dopaminergic neurons and is a causative gene within DOPA-responsive dystonia and Parkinson's Disease [79,80]. GCH1 has also been shown to be involved in pain regulation/sensitisation, through levels of BH_4 regulating the activity of nitric oxide synthases and tyrosine/tryptophan hydroxylases, which when inhibiting or blocking GCH1 can be an effective anti-neuropathic treatment [81,82]. This therefore may implicate the Punch-BH_4-AP-1 interaction and may have implications outside of redox regulation, for example in blocking BH_4 production to reduce pain levels and when unblocked allows for the pain response to occur.

Mutations within GTPCH1 lead to the reduced synthesis of BH_4, which therefore leads to the limited synthesis of dopamine and nitric oxide. This not only has impacts on redox regulation as shown in our study (Figure 4.2D) but impacts the levels of TH and dopamine which further impacts the interactions of our hypothesis model. Previous studies have shown that TH interacts with GTPCH1 to prevent BH_4 inhibition, which adds further regulation into our model hypothesis [49]. The administration of BH_4 could not restore TH activity, which is required for dopamine synthesis, if the GTPCH1 was mutated which suggests not only must normal BH_4 levels be required for TH synthesis, but normal GTPCH1 function must also be present for maximum TH activity to occur [49]. This may identify why levels of ROS continued to be high within our DHFR rescues of the *Punch* mutants in Figure 4.4D, since even though BH_4 levels were rescued, the mutated Punch prevented the maximum activity of TH and therefore maximum synthesis of dopamine while aso failing to generate an AP-1 response of the appropriate level. Dopamine is an unstable molecule that may auto-oxidise to generate hydrogen peroxide, therefore further reducing levels of dopamine and contributing to Parkinson's pathology [83]. Too high levels of BH_4 has implications in the pathophysiology of ischemic neuronal death [84]. One product of BH_4 is nitric oxide (NO), which has been shown to aggravate neuronal injury and leads to NOS activation, along with producing higher levels of dopamine which in excess will produce hydrogen peroxide. The increase in BH_4 levels plays a role in not only increasing these levels of ROS and NOS but reduces AP-1 activity, reducing the antioxidant response and therefore reduced regulation of oxidative stress.

These past studies do explain some of the questions that have arisen from our results. The increase in ROS within our *Punch* mutants in Figure 4.2D may be due to reduced dopamine synthesis and therefore degradation along with the reduced activity of TH, leading to an increase in ROS even though AP-1 is dissociated and activating an antioxidative response. The increased ROS levels within our DHFR rescues of *Punch* heterozygotes in Figure 4.4D may be due to the increased levels of BH_4 producing high levels of NO and leading to NOS activation and neuronal injury, leading to an increase in ROS along with the inhibition of AP-1 activity. This further puts into perspective the highly regulated interaction required between GTPCH1, AP-1 and BH_4 levels to allow not only a carefully regulated antioxidant response, but to ensure TH activity and dopamine balance is also regulated. This interaction may also have implications with the numerous other proteins that interact with GTPCH1, including TH, which may implicate an even further regulation within this interaction.

The restraint of JNK/AP-1 activation through interactions with proteins has a history in redox regulation and activation. For example, apoptosis signal-regulating kinase 1 (ASK1), which is required for the sustained activation of JNK, is directly inhibited by thioredoxin which leads to reduced activity of ASK1 and JNK [34,85]. JNK itself has also been shown to be regulated through a dose-dependent inhibition by glutathione S-transferase Pi (GSTp) [33]. The regulation of proteins through direct inhibition has been shown in numerous studies, each with roles in redox regulation and activation, to which our work identifies a novel rheostat-like mechanism to regulate AP-1 activity, expanding and developing upon this mechanism.

5.3 Final remarks and future of work

To conclude the work, a potential novel interaction between Punch and AP-1 has been characterised which may act as a redox regulator within the *Drosophila* nervous system. This interaction is regulated by the levels of BH_4 present. Excess BH_4 which is present in normal, physiological levels of ROS, is proposed to promote the association of Punch and AP-1, preventing the synthesis of BH_4 and the transcriptional activity of AP-1 and therefore no antioxidant response. When ROS levels rise to a pathological level, the BH_4 is readily oxidised, allowing the dissociation of Punch and AP-1, leading to the synthesis of BH_4 and the transcription of an antioxidant response. The use of the *Drosophila* system, including NMJ analysis, measurements of ROS levels and cell biology along with bioinformatics throughout this project and previous studies conducted by Nathan Garnham have identified this interaction, and showing the impacts of *Punch* mutations on synapse overgrowth and ROS levels, which may have implications in neurodegenerative diseases. Previous studies have shown mutations in GTPCH1 is a cause for the development of DOPA-responsive dystonia and Parkinson's Disease [79]. We attempted to rescue the impacts of the *Punch* and mutations by manipulating levels of BH_4 using *DHFR* overexpression, which did rescue the synapse overgrowth but did not rescue the increased ROS levels. This implicates this interaction and all the components present must all be equally regulated to ensure an accurate antioxidant response can be achieved.

Although we have identified this novel interaction, there are still many factors that surround this that must be considered and investigated. Other proteins have been shown to interact with GTPCH1 which may further regulate this protein which needs to be considered within this model. Tyrosine hydroxylase has been shown to inhibit the inhibition caused by excess BH_4 which may have a part within our model hypothesis [49]. Potential experiments that could be conducted to investigate this are pull-downs, similar to the ones conducted by Nathan

Garnham, where we tag either Jra/Kayak or Punch and pull down these different proteins including TH and see if the levels change in conditions of excess or no BH_4. Experimentation into measuring the levels of BH_4 within the *Punch* mutants and within the DHFR rescues to confirm the role BH_4 plays within this model acting as a redox signaling molecule. The potential use of high-performance liquid chromatography could be used to detect the levels of BH_4 within these flies, however the methods to prevent the oxidation of BH_4 must be investigated [86,87]. The ability to accurately measure BH_4 levels will help to investigate how BH_4 plays a part within this interaction, if through direct inhibition of AP-1/Punch similar to ASK1-Thioredoxin or a dose-dependent inhibition similar to JNK-GSTp [33,85]. This would also aid in investigating the impacts of *Punch* heterozygous mutations, to see if the interaction of AP-1, Punch and BH_4 is impacted or the levels of BH_4 are dysregulated leading to reduced regulation. Even though a new, novel redox regulating mechanism has been proposed within the *Drosophila* system, there are still many factors that surround it that must be investigated, both within the *Drosophila* and mammalian systems, to further understand and potentially identify a therapeutic pathway for the treatment of DOPA-responsive dystonia and Parkinson's Disease caused by the mutations within GTPCH1.

Supplementary Data

Table S1. Raw and normalised bouton counts for NMJ analysis

Genotype and Condition	Raw Bouton ± SEM	MSA ± SEM (μm^2)	Normalised Bouton	N
Figure 3.6 Reducing Punch levels releases AP-1 to drive synapse overgrowth under conditions of oxidative stress				
WT	44 ± 1.476	72534 ± 2713	NS	14
$Pu^{EY2616A}$/WT	46 ± 2.130	71999 ± 2677	48 ± 3.148	14
Pu^{R1}/WT	44 ± 2.356	75666 ± 2503	43 ± 2.662	15
WT 10% Ethanol	48 ± 2.560	73934 ± 2077	48 ± 2.657	12
$Pu^{EY2616A}$/WT 10% Ethanol	69 ± 2.492	71959 ± 2151	71 ± 3.190	17
Pu^{R1}/WT 10% Ethanol	68 ± 4.109	69792 ± 4214	74 ± 5.956	13
WT 10mM Trolox	39 ± 2.467	71752 ± 2991	41 ± 3.564	11
$Pu^{EY2616A}$/WT 10mM Trolox	48 ± 3.018	74234 ± 3105	47 ± 2.820	11
Pu^{R1}/WT 10mM Trolox	47 ± 1.615	77803 ± 2233	44 ± 1.759	14
Figure 3.7 Oxidative stress via DEM does not further induce synaptic overgrowth within Punch heterozygotes				
WT 10% Ethanol	48 ± 2.560	73934 ± 2077	NS	14
$Pu^{EY2616A}$/WT 10% Ethanol	69 ± 2.492	71959 ± 2151	72 ± 3.251	13
Pu^{R1}/WT 10% Ethanol	68 ± 4.109	69792 ± 4214	75 ± 6.071	13
WT 10mM DEM	65 ± 3.115	64488 ± 2673	77 ± 4.714	14
$Pu^{EY2616A}$/WT 10mM DEM	74 ± 3.894	70550 ± 1966	77 ± 3.742	13
Pu^{R1}/WT 10mM DEM	73 ± 4.091	67611 ± 2139	81 ± 5.059	12
WT 10mM Trolox + 10mM DEM	39 ± 2.438	67325 ± 3203	41 ± 2.475	11
$Pu^{EY2616A}$/WT 10mM Trolox + 10mM DEM	45 ± 2.419	67419 ± 2614	50 ± 2.419	14
Pu^{R1}/WT 10mM Trolox + 10mM DEM	45 ± 2.039	77514 ± 2145	43 ± 1.980	16
Figure 3.8 Raising BH_4 levels rescues synaptic overgrowth when Punch levels are reduced				
WT 10% Ethanol	48 ± 2.560	73934 ± 2077	NS	14
$Pu^{EY2616A}$/WT 10% Ethanol	69 ± 2.492	71959 ± 2151	72 ± 3.251	13
Pu^{R1}/WT 10% Ethanol	68 ± 4.109	69792 ± 4214	75 ± 6.071	13
$Pu^{EY2616A}$/+:SPIN>DHFR 10% Ethanol	44 ± 2.005	81896 ± 2500	40 ± 2.203	14
Pu^{R1}/+:SPIN>DHFR 10% Ethanol	42 ± 1.376	79896 ± 1712	39 ± 1.217	13
WT 10mM DEM	65 ± 3.115	64488 ± 2673	77 ± 4.714	16
$Pu^{EY2616A}$/WT 10mM DEM	74 ± 3.894	70550 ± 1966	77 ± 3.742	13
Pu^{R1}/WT 10mM DEM	73 ± 4.091	67611 ± 2139	81 ± 5.059	12
$Pu^{EY2616A}$/+:SPIN>DHFR 10mM DEM	51 ± 2.692	77665 ± 3328	50 ± 3.156	15
Pu^{R1}/+:SPIN>DHFR 10mM DEM	46 ± 1.911	74732 ± 2542	46 ± 2.202	16
Figure 3.9 Raising BH_4 levels rescues synaptic overgrowth within *hiw* mutants				
WT	51 ± 2.275	85611 ± 1107	NS	16
nSyb>Pu	49 ± 1.909	81128 ± 1669	51 ± 1.851	12
nSyb>DHFR	51 ± 2.742	80690 ± 1366	54 ± 3.218	10
HIW^{ND9}	97 ± 6.766	75213 ± 2708	112 ± 9.658	10
HIW^{ND9}:nSyb>Pu	56 ± 2.107	83596 ± 1476	58 ± 2.231	16
HIW^{ND9}:nSyb>DHFR	58 ± 4.066	79442 ± 2056	62 ± 4.113	12

Table S2. Raw branch number counts for NMJ analysis

Genotype and Condition	Raw Branch Number ±SEM	MSA ± SEM (μm^2)	N
Figure 3.6 Reducing Punch levels releases AP-1 to drive synapse overgrowth under conditions of oxidative stress			
WT	4.86 ± 0.231	72534 ± 2713	14
$Pu^{EY2616A}$/WT	5.53 ± 0.413	71999 ± 2677	14
Pu^{R1}/WT	5.06 ± 0.378	75666 ± 2503	15
WT 10% Ethanol	7.64 ± 0.599	73934 ± 2077	12
$Pu^{EY2616A}$/WT 10% Ethanol	9.08 ± 0.487	71959 ± 2151	17
Pu^{R1}/WT 10% Ethanol	8.92 ± 0.593	69792 ± 4214	13
WT 10mM Trolox	5.64 ± 0.664	71752 ± 2991	11
$Pu^{EY2616A}$/WT 10mM Trolox	4.91 ± 0.653	74234 ± 3105	11
Pu^{R1}/WT 10mM Trolox	5.07 ± 0.267	77803 ± 2233	14
Figure 3.7 Oxidative stress via DEM does not further induce synaptic overgrowth within Punch heterozygotes			
WT 10% Ethanol	7.64 ± 0.599	73934 ± 2077	14
$Pu^{EY2616A}$/WT 10% Ethanol	9.08 ± 0.487	71959 ± 2151	13
Pu^{R1}/WT 10% Ethanol	8.92 ± 0.593	69792 ± 4214	13
WT 10mM DEM	10.7 ± 0.496	64488 ± 2673	14
$Pu^{EY2616A}$/WT 10mM DEM	11.4 ± 0.712	70550 ± 1966	13
Pu^{R1}/WT 10mM DEM	10.0 ± 0.707	67611 ± 2139	12
WT 10mM Trolox + 10mM DEM	3.09 ± 0.315	67325 ± 3203	11
$Pu^{EY2616A}$/WT 10mM Trolox + 10mM DEM	4.14 ± 0.177	67419 ± 2614	14
Pu^{R1}/WT 10mM Trolox + 10mM DEM	4.63 ± 0.301	77514 ± 2145	16
Figure 3.8 Raising BH_4 levels rescues synaptic overgrowth when Punch levels are reduced			
WT 10% Ethanol	7.64 ± 0.599	73934 ± 2077	14
$Pu^{EY2616A}$/WT 10% Ethanol	9.08 ± 0.487	71959 ± 2151	13
Pu^{R1}/WT 10% Ethanol	8.92 ± 0.593	69792 ± 4214	13
$Pu^{EY2616A}$/+:SPIN>DHFR 10% Ethanol	5.92 ± 0.487	81896 ± 2500	14
Pu^{R1}/+:SPIN>DHFR 10% Ethanol	5.07 ± 0.419	79896 ± 1712	13
WT 10mM DEM	10.7 ± 0.496	64488 ± 2673	16
$Pu^{EY2616A}$/WT 10mM Trolox + 10mM DEM	4.14 ± 0.177	67419 ± 2614	14
Pu^{R1}/WT 10mM Trolox + 10mM DEM	4.63 ± 0.301	77514 ± 2145	16
$Pu^{EY2616A}$/+:SPIN>DHFR 10mM DEM	6.31 ± 0.522	77665 ± 3328	15
Pu^{R1}/+:SPIN>DHFR 10mM DEM	4.81 ± 0.421	74732 ± 2542	16
Figure 3.9 Raising BH_4 levels rescues synaptic overgrowth within *hiw* mutants			
WT	3.75 ± 0.310	85611 ± 1107	16
nSyb>Pu	3.58 ± 0.260	81128 ± 1669	12
nSyb>DHFR	4.10 ± 0.348	80690 ± 1366	10
HIW^{ND9}	8.50 ± 0.792	75213 ± 2708	10
HIW^{ND9}:nSyb>Pu	4.50 ± 0.365	83596 ± 1476	16
HIW^{ND9}:nSyb>DHFR	4.75 ± 0.509	79442 ± 2056	12

Table S3. Raw and normalised synapse length for NMJ analysis

Genotype and Condition	Raw NMJ Length ± SEM (µm)	MSA ± SEM ($µm^2$)	Normalised NMJ Length (µm)	N
Figure 3.6 Reducing Punch levels releases AP-1 to drive synapse overgrowth under conditions of oxidative stress				
WT (W-)	307 ± 8.062	72534 ± 2713	NS	14
$Pu^{EY2616A}$/WT	317 ± 8.576	71999 ± 2677	326 ± 14.93	14
Pu^{R1}/WT	377 ± 21.49	75666 ± 2503	369 ± 24.83	15
WT 10% Ethanol	490 ± 29.52	73934 ± 2077	482 ± 26.216	12
$Pu^{EY2616A}$/WT 10% Ethanol	459 ± 19.12	71959 ± 2151	467 ± 22.95	17
Pu^{R1}/WT 10% Ethanol	624 ± 66.74	69792 ± 4214	668 ± 74.09	13
WT 10mM Trolox	369 ± 23.05	71752 ± 2991	378 ± 24.73	11
$Pu^{EY2616A}$/WT 10mM Trolox	476 ± 29.92	74234 ± 3105	468 ± 27.52	11
Pu^{R1}/WT 10mM Trolox	477 ± 19.18	77803 ± 2233	445 ± 12.72	14
Figure 3.7 Oxidative stress via DEM does not further induce synaptic overgrowth within Punch heterozygotes				
WT 10% Ethanol	490 ± 29.52	73934 ± 2077	NS	14
$Pu^{EY2616A}$/WT 10% Ethanol	459 ± 19.12	71959 ± 2151	476 ± 23.39	13
Pu^{R1}/WT 10% Ethanol	624 ± 66.74	69792 ± 4214	680 ± 75.52	13
WT 10mM DEM	565 ± 27.55	64488 ± 2673	668 ± 46.65	14
$Pu^{EY2616A}$/WT 10mM DEM	464 ± 38.21	70550 ± 1966	484 ± 35.22	13
Pu^{R1}/WT 10mM DEM	647 ± 35.72	67611 ± 2139	723 ± 57.88	12
WT 10mM Trolox + 10mM DEM	300 ± 17.35	67325 ± 3203	340 ± 28.20	11
$Pu^{EY2616A}$/WT 10mM Trolox + 10mM DEM	458 ± 30.06	67419 ± 2614	510 ± 35.84	14
Pu^{R1}/WT 10mM Trolox + 10mM DEM	465 ± 15.93	77514 ± 2145	448 ± 19.32	16
Figure 3.8 Raising BH_4 levels rescues synaptic overgrowth when Punch levels are reduced				
WT 10% Ethanol	490 ± 29.52	73934 ± 2077	NS	14
$Pu^{EY2616A}$/WT 10% Ethanol	459 ± 19.12	71959 ± 2151	476 ± 23.39	13
Pu^{R1}/WT 10% Ethanol	624 ± 66.74	69792 ± 4214	680 ± 75.52	13
$Pu^{EY2616A}$/+:SPIN>DHFR 10% Ethanol	460 ± 18.18	81896 ± 2500	417 ± 15.08	14
Pu^{R1}/+:SPIN>DHFR 10% Ethanol	472 ± 16.51	79896 ± 1712	439 ± 17.25	13
WT 10mM DEM	565 ± 27.55	64488 ± 2673	668 ± 46.65	16
$Pu^{EY2616A}$/WT 10mM Trolox + 10mM DEM	458 ± 30.06	67419 ± 2614	510 ± 35.84	14
Pu^{R1}/WT 10mM Trolox + 10mM DEM	465 ± 15.93	77514 ± 2145	448 ± 19.32	16
$Pu^{EY2616A}$/+:SPIN>DHFR 10mM DEM	588 ± 23.99	77665 ± 3328	571 ± 28.13	15
Pu^{R1}/+:SPIN>DHFR 10mM DEM	506 ± 26.68	74732 ± 2542	501 ± 22.33	16
Figure 3.9 Raising BH_4 levels rescues synaptic overgrowth within *hiw* mutants				
WT	499 ± 22.01	85611 ± 1107	NS	16
nSyb>Pu	450 ± 10.80	81128 ± 1669	477 ± 15.38	12
nSyb>DHFR	534 ± 28.15	80690 ± 1366	568 ± 31.47	10
HIW^{ND9}	1065 ± 56.84	75213 ± 2708	1230 ± 88.37	10
HIW^{ND9}:nSyb>Pu	666 ± 28.91	83596 ± 1476	684 ± 30.13	16
HIW^{ND9}:nSyb>DHFR	670 ± 43.91	79442 ± 2056	724 ± 43.91	12

Table S4. Western Blot gel components and volumes used during investigation

	Stacking Gel (4%)	Resolving Gel (10%)
30% Acrylamide	1.98ml	5ml
0.5M Tris HCl pH 6.8	3.78ml	X
1.5M Tris HCl pH 8.8	X	3.75ml
10% SDS	150µl	150µl
dH_2O	9ml	6ml
TEMED	15µl	7.5µl
10% APS	75µl	75µl

Figure S1. Control experiments for larval brain colocalisation dissection experiment

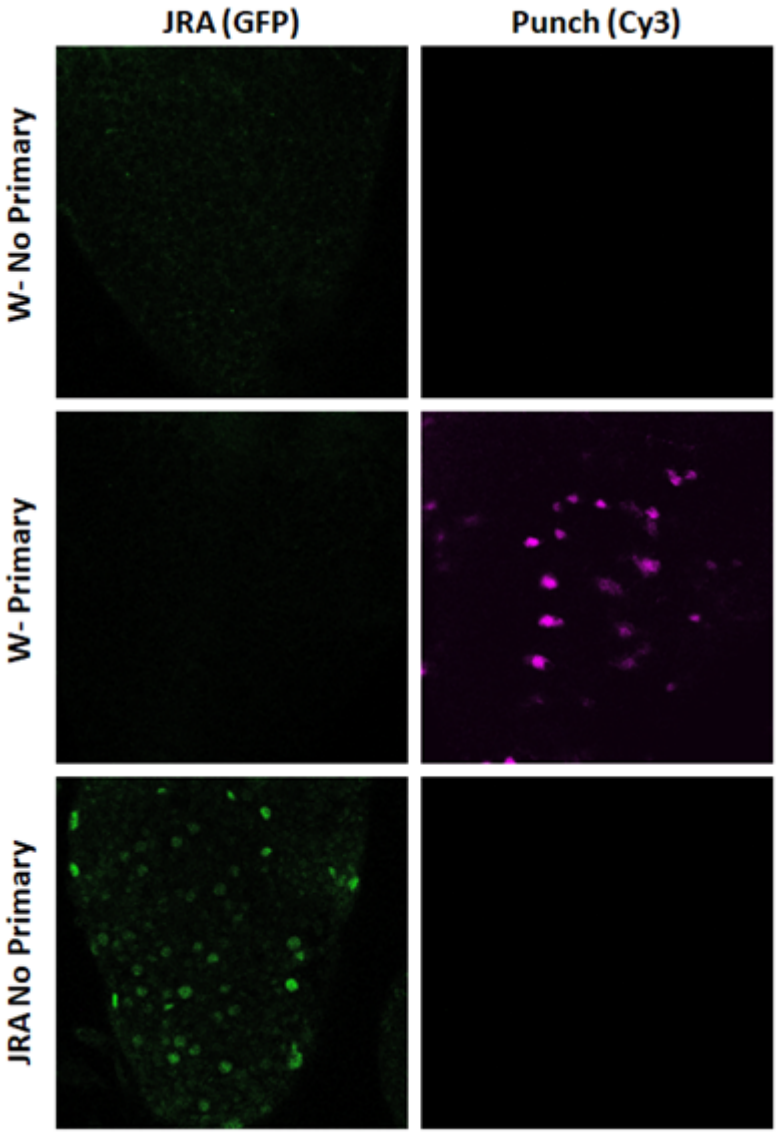

References

1. Isaksson, C., Sheldon, B. C. & Uller, T. The Challenges of Integrating Oxidative Stress into Life-history Biology. *Bioscience* **61**, 194–202 (2011).
2. Zhou, L. Z.-H., Johnson, A. P. & Rando, T. A. NFκB and AP-1 mediate transcriptional responses to oxidative stress in skeletal muscle cells. *Free Radical Biology and Medicine* **31**, 1405–1416 (2001).
3. Partridge, L. The new biology of ageing. *Philos. Trans. R. Soc. Lond. B Biol. Sci.* **365**, 147–154 (2010).
4. Davalli, P., Mitic, T., Caporali, A., Lauriola, A. & D'Arca, D. ROS, Cell Senescence, and Novel Molecular Mechanisms in Aging and Age-Related Diseases. *Oxid. Med. Cell. Longev.* **2016**, 3565127 (2016).
5. Liguori, I. *et al.* Oxidative stress, aging, and diseases. *Clin. Interv. Aging* **13**, 757–772 (2018).
6. Bishop, N. A., Lu, T. & Yankner, B. A. Neural mechanisms of ageing and cognitive decline. *Nature* **464**, 529–535 (2010).
7. Sanz, A. OP-20 - Mitochondrial ROS and ageing. *Free Radical Biology and Medicine* **108**, S9 (2017).
8. Salim, S. Oxidative Stress and the Central Nervous System. *J. Pharmacol. Exp. Ther.* **360**, 201–205 (2017).
9. Mattson, M. P. & Arumugam, T. V. Hallmarks of Brain Aging: Adaptive and Pathological Modification by Metabolic States. *Cell Metab.* **27**, 1176–1199 (2018).
10. Uttara, B., Singh, A. V., Zamboni, P. & Mahajan, R. T. Oxidative stress and neurodegenerative diseases: a review of upstream and downstream antioxidant therapeutic options. *Curr. Neuropharmacol.* **7**, 65–74 (2009).
11. Wang, X. & Michaelis, E. K. Selective neuronal vulnerability to oxidative stress in the brain. *Front. Aging Neurosci.* **2**, 12 (2010).
12. Sharma, P., Jha, A. B., Dubey, R. S. & Pessarakli, M. Reactive Oxygen Species, Oxidative Damage, and Antioxidative Defense Mechanism in Plants under Stressful

Conditions. *J. Bot.* **2012**, (2012).

13. Ray, P. D., Huang, B.-W. & Tsuji, Y. Reactive oxygen species (ROS) homeostasis and redox regulation in cellular signaling. *Cell. Signal.* **24**, 981–990 (2012).
14. Auten, R. L. & Davis, J. M. Oxygen Toxicity and Reactive Oxygen Species: The Devil Is in the Details. *Pediatr. Res.* **66**, 121–127 (2009).
15. Bae, Y. S., Oh, H., Rhee, S. G. & Yoo, Y. D. Regulation of reactive oxygen species generation in cell signaling. *Mol. Cells* **32**, 491–509 (2011).
16. Milton, V. J. & Sweeney, S. T. Oxidative stress in synapse development and function. *Dev. Neurobiol.* **72**, 100–110 (2012).
17. Schieber, M. & Chandel, N. S. ROS function in redox signaling and oxidative stress. *Curr. Biol.* **24**, R453–62 (2014).
18. Giridharan, S. S. P., Rohn, J. L., Naslavsky, N. & Caplan, S. Differential regulation of actin microfilaments by human MICAL proteins. *J. Cell Sci.* **125**, 614–624 (2012).
19. Liu, Z., Zhou, T., Ziegler, A. C., Dimitrion, P. & Zuo, L. Oxidative Stress in Neurodegenerative Diseases: From Molecular Mechanisms to Clinical Applications. *Oxid. Med. Cell. Longev*, 2525967 (2017).
20. Pizzino, G. *et al.* Oxidative Stress: Harms and Benefits for Human Health. *Oxid. Med. Cell. Longev*, 8416763 (2017).
21. Gandhi, S. & Abramov, A. Y. Mechanism of Oxidative Stress in Neurodegeneration. *Oxid. Med. Cell. Longev*, (2012).
22. Trist, B., Hilton, J. B., Crouch, P. J., Hare, D. J. & Double, K. L. Superoxide dismutase 1 in health and disease: How a front-line antioxidant becomes neurotoxic. *Angew. Chem. Int. Ed Engl.* **n/a**, (2020).
23. Collet, J.-F. & Messens, J. Structure, function, and mechanism of thioredoxin proteins. *Antioxid. Redox Signal.* **13**, 1205–1216 (2010).
24. Oswald, M. C. W., Garnham, N., Sweeney, S. T. & Landgraf, M. Regulation of neuronal development and function by ROS. *FEBS Lett.* **592**, 679–691 (2018).

25. Krysan, K. & Lou, M. F. Regulation of human thioltransferase (hTTase) gene by AP-1 transcription factor under oxidative stress. *Invest. Ophthalmol. Vis. Sci.* **43**, 1876–1883 (2002).
26. Baxter, P. S. & Hardingham, G. E. Adaptive regulation of the brain's antioxidant defences by neurons and astrocytes. *Free Radical Biology and Medicine* vol. 100 147–152 (2016).
27. Hess, J., Angel, P. & Schorpp-Kistner, M. AP-1 subunits: quarrel and harmony among siblings. *J. Cell Sci.* **117**, 5965–5973 (2004).
28. Hartwig, C. L., Worrell, J., Levine, R. B., Ramaswami, M. & Sanyal, S. Normal dendrite growth in Drosophila motor neurons requires the AP-1 transcription factor. *Dev. Neurobiol.* **68**, 1225–1242 (2008).
29. Tuvikene, J., Pruunsild, P., Orav, E., Esvald, E.-E. & Timmusk, T. AP-1 Transcription Factors Mediate BDNF-Positive Feedback Loop in Cortical Neurons. *J. Neurosci.* **36**, 1290–1305 (2016).
30. Ugbode, C. *et al.* JNK signalling regulates antioxidant responses in neurons. *Redox Biol* **37**, 101712 (2020).
31. Milton, V. J. *et al.* Oxidative stress induces overgrowth of the Drosophila neuromuscular junction. *Proc. Natl. Acad. Sci. U. S. A.* **108**, 17521–17526 (2011).
32. Garnham, N. Dissecting the role of JNK/AP-1 signaling in the regulation of redox homeostasis within neurons. (University of York, 2016).
33. Adler, V. *et al.* Regulation of JNK signaling by GSTp. *EMBO J.* **18**, 1321–1334 (1999).
34. Saitoh, M. *et al.* Mammalian thioredoxin is a direct inhibitor of apoptosis signal-regulating kinase (ASK) 1. *EMBO J.* **17**, 2596–2606 (1998).
35. Kim, K., Kim, H. & Yim, J. Functional analysis of sepiapterin reductase in Drosophila melanogaster. *Pteridines* **26**, 63–68 (2015).
36. Guibal, P. *et al.* Simultaneous determination of all forms of biopterin and neopterin in cerebrospinal fluid. *ACS Chem. Neurosci.* **5**, 533–541 (2014).

37. Bailey, J. *et al.* A novel role for endothelial tetrahydrobiopterin in mitochondrial redox balance. *Free Radic. Biol. Med.* **104**, 214–225 (2017).
38. Base, K., Lombard, W. W., Karhausen, J., Sheng, H. & Spasojevic, I. Quantification of Tetrahydrobiopterin (BH4), Dihydrobiopterin (BH2) and Biopterin (BP) in Mouse Brain and Intestines After Ischemic Injury by Liquid Chromatography-Electrospray Tandem Mass Spectrometry (LC-ESI-MS/MS). *Free Radical Biology and Medicine* **53**, S16 (2012).
39. Yuan, T.-F., Huang, H.-Q., Gao, L., Wang, S.-T. & Li, Y. A novel and reliable method for tetrahydrobiopterin quantification: Benzoyl chloride derivatization coupled with liquid chromatography-tandem mass spectrometry analysis. *Free Radic. Biol. Med.* **118**, 119–125 (2018).
40. He, A. & Rosazza, J. P. N. GTP cyclohydrolase I: purification, characterization, and effects of inhibition on nitric oxide synthase in nocardia species. *Appl. Environ. Microbiol.* **69**, 7507–7513 (2003).
41. Chen, W. *et al.* Role of increased guanosine triphosphate cyclohydrolase-1 expression and tetrahydrobiopterin levels upon T cell activation. *J. Biol. Chem.* **286**, 13846–13851 (2011).
42. Reynolds, E. R. & O'Donnell, J. M. Characterization of new Punch mutations: identification of two additional mutant classes. *Genetics* **119**, 609–617 (1988).
43. Chen, X., Reynolds, E. R., Ranganayakulu, G. & O'Donnell, J. M. A maternal product of the Punch locus of Drosophila melanogaster is required for precellular blastoderm nuclear divisions. *J. Cell Sci.* **107 (Pt 12)**, 3501–3513 (1994).
44. Kapatos, G., Hirayama, K., Shimoji, M. & Milstien, S. GTP cyclohydrolase I feedback regulatory protein is expressed in serotonin neurons and regulates tetrahydrobiopterin biosynthesis. *J. Neurochem.* **72**, 669–675 (1999).
45. McLean, J. R., Krishnakumar, S. & O'Donnell, J. M. Multiple mRNAs from the Punch locus of Drosophila melanogaster encode isoforms of GTP cyclohydrolase I with distinct

N-terminal domains. *J. Biol. Chem.* **268**, 27191–27197 (1993).

46. Bowling, K. M. *et al.* Direct binding of GTP cyclohydrolase and tyrosine hydroxylase: regulatory interactions between key enzymes in dopamine biosynthesis. *J. Biol. Chem.* **283**, 31449–31459 (2008).
47. Krim, E. *et al.* Mutation in the GCH1 gene with dopa-responsive dystonia and phenotypic variability. *Neurol Genet* **4**, e231 (2018).
48. Hyland, K. Inherited disorders affecting dopamine and serotonin: critical neurotransmitters derived from aromatic amino acids. *J. Nutr.* **137**, 1568S–1572S; discussion 1573S–1575S (2007).
49. Meiser, J., Weindl, D. & Hiller, K. Complexity of dopamine metabolism. *Cell Commun. Signal.* **11**, 34 (2013).
50. Choi, H. J., Kim, S. W., Lee, S. Y. & Hwang, O. Dopamine-dependent cytotoxicity of tetrahydrobiopterin: a possible mechanism for selective neurodegeneration in Parkinson's disease. *J. Neurochem.* **86**, 143–152 (2003).
51. Crabtree, M. J. & Channon, K. M. Synthesis and recycling of tetrahydrobiopterin in endothelial function and vascular disease. *Nitric Oxide* **25**, 81–88 (2011).
52. Witzemann, V. Development of the neuromuscular junction. *Cell Tissue Res.* **326**, 263–271 (2006).
53. Sanyal, S., Sandstrom, D. J., Hoeffer, C. A. & Ramaswami, M. AP-1 functions upstream of CREB to control synaptic plasticity in Drosophila. *Nature* **416**, 870–874 (2002).
54. Sanyal, S., Narayanan, R., Consoulas, C. & Ramaswami, M. Evidence for cell autonomous AP1 function in regulation of Drosophila motor-neuron plasticity. *BMC Neurosci.* **4**, 20 (2003).
55. Oswald, M. C. *et al.* Reactive oxygen species regulate activity-dependent neuronal plasticity in Drosophila. *Elife* **7**, (2018).
56. Jennings, B. H. Drosophila – a versatile model in biology & medicine. *Mater. Today* **14**, 190–195 (2011).

57. Yadav, R., Chanu, S. I., Raj, K., Nisha & Sarkar, S. Drosophila melanogaster: A Prime Experimental Model System for Aging Studies. in *Topics in Biomedical Gerontology* (eds. Rath, P. C., Sharma, R. & Prasad, S.) 3–33 (Springer Singapore, 2017).
58. Pandey, U. B. & Nichols, C. D. Human disease models in Drosophila melanogaster and the role of the fly in therapeutic drug discovery. *Pharmacol. Rev.* **63**, 411–436 (2011).
59. Mirzoyan, Z. *et al.* Drosophila melanogaster: A Model Organism to Study Cancer. *Front. Genet.* **10**, 51 (2019).
60. Tolwinski, N. S. Introduction: Drosophila-A Model System for Developmental Biology. *J Dev Biol* **5**, (2017).
61. Brent, J. R., Werner, K. M. & McCabe, B. D. Drosophila larval NMJ dissection. *J. Vis. Exp.* (2009) doi:10.3791/1107.
62. Piper, M. D. W. & Partridge, L. Drosophila as a model for ageing. *Biochim. Biophys. Acta Mol. Basis Dis.* **1864**, 2707–2717 (2018).
63. Sang, T.-K. & Jackson, G. R. Drosophila models of neurodegenerative disease. *NeuroRx* **2**, 438–446 (2005).
64. Wan, H. I. *et al.* Highwire regulates synaptic growth in Drosophila. *Neuron* **26**, 313–329 (2000).
65. Stelzer, G. *et al.* The GeneCards Suite: From Gene Data Mining to Disease Genome Sequence Analyses. *Curr. Protoc. Bioinformatics* **54**, 1.30.1–1.30.33 (2016).
66. Vierbuchen, T. *et al.* AP-1 Transcription Factors and the BAF Complex Mediate Signal-Dependent Enhancer Selection. *Mol. Cell* **68**, 1067–1082.e12 (2017).
67. Fishilevich, S. *et al.* GeneHancer: genome-wide integration of enhancers and target genes in GeneCards. *Database* **2017**, (2017).
68. Kockel, L., Homsy, J. G. & Bohmann, D. Drosophila AP-1: lessons from an invertebrate. *Oncogene* **20**, 2347–2364 (2001).
69. Jindra, M. *et al.* Coactivator MBF1 preserves the redox-dependent AP-1 activity during oxidative stress in Drosophila. *EMBO J.* **23**, 3538–3547 (2004).

70. Foppoli, C. & Perluigi, M. Chapter 9 - Redox-dependent mechanisms of carcinogenesis in human papillomavirus infection. in *Cancer (Second Edition)* (eds. Preedy, V. R. & Patel, V. B.) 87–100 (Academic Press, 2021).
71. Szalóki, N., Krieger, J. W., Komáromi, I., Tóth, K. & Vámosi, G. Evidence for Homodimerization of the c-Fos Transcription Factor in Live Cells Revealed by Fluorescence Microscopy and Computer Modeling. *Mol. Cell. Biol.* **35**, 3785–3798 (2015).
72. Collins, C. A., Wairkar, Y. P., Johnson, S. L. & DiAntonio, A. Highwire restrains synaptic growth by attenuating a MAP kinase signal. *Neuron* **51**, 57–69 (2006).
73. Peng, J.-J. *et al.* A circuit-dependent ROS feedback loop mediates glutamate excitotoxicity to sculpt the Drosophila motor system. *Elife* **8**, (2019).
74. Sweeney, S. T. & Davis, G. W. Unrestricted synaptic growth in spinster-a late endosomal protein implicated in TGF-beta-mediated synaptic growth regulation. *Neuron* **36**, 403–416 (2002).
75. Wu, C., Wairkar, Y. P., Collins, C. A. & DiAntonio, A. Highwire function at the Drosophila neuromuscular junction: spatial, structural, and temporal requirements. *J. Neurosci.* **25**, 9557–9566 (2005).
76. Le Guyader, S., Maier, J. & Jesuthasan, S. Esrom, an ortholog of PAM (protein associated with c-myc), regulates pteridine synthesis in the zebrafish. *Dev. Biol.* **277**, 378–386 (2005).
77. Du, J. *et al.* Identification of proteins interacting with GTP cyclohydrolase I. *Biochem. Biophys. Res. Commun.* **385**, 143–147 (2009).
78. Reynolds, E. R. & O'Donnell, J. M. An analysis of the embryonic defects in Punch mutants of Drosophila melanogaster. *Dev. Biol.* **123**, 430–441 (1987).
79. Ichinose, H., Nomura, T. & Sumi-Ichinose, C. Metabolism of tetrahydrobiopterin: its relevance in monoaminergic neurons and neurological disorders. *Chem. Rec.* **8**, 378–385 (2008).

80. Yoshino, H. *et al.* GCH1 mutations in dopa-responsive dystonia and Parkinson's disease. *J. Neurol.* **265**, 1860–1870 (2018).
81. Latremoliere, A. & Costigan, M. GCH1, BH4 and pain. *Curr. Pharm. Biotechnol.* **12**, 1728–1741 (2011).
82. Tegeder, I. *et al.* GTP cyclohydrolase and tetrahydrobiopterin regulate pain sensitivity and persistence. *Nat. Med.* **12**, 1269–1277 (2006).
83. Weng, M. *et al.* The Sources of Reactive Oxygen Species and Its Possible Role in the Pathogenesis of Parkinson's Disease. *Parkinson's Disease* **2018**, (2018).
84. Cho, S. *et al.* Blockade of tetrahydrobiopterin synthesis protects neurons after transient forebrain ischemia in rat: a novel role for the cofactor. *J. Neurosci.* **19**, 878–889 (1999).
85. Tobiume, K. *et al.* ASK1 is required for sustained activations of JNK/p38 MAP kinases and apoptosis. *EMBO Rep.* **2**, 222–228 (2001).
86. Edgar, K. S., Galvin, O. M., Collins, A., Katusic, Z. S. & McDonald, D. M. BH4-Mediated Enhancement of Endothelial Nitric Oxide Synthase Activity Reduces Hyperoxia-Induced Endothelial Damage and Preserves Vascular Integrity in the Neonate. *Invest. Ophthalmol. Vis. Sci.* **58**, 230–241 (2017).
87. Zhao, Y. *et al.* Detection of tetrahydrobiopterin by LC-MS/MS in plasma from multiple species. *Bioanalysis* **1**, 895–903 (2009).